International Doctorate Program in Molecular Oncology and Endocrinology
Doctorate School in Molecular Medicine

XIX cycle - 2003–2007
Coordinator: Prof. Giancarlo Vecchio

“Analysis of oncolytic adenovirus *dl*922-947 effects on anaplastic thyroid carcinoma cells (ATC) and potential therapeutic associations”

Irma Iacuzzo

University of Naples Federico II
Dipartimento di Biologia e Patologia Cellulare e Molecolare “L. Califano”

Administrative Location

Dipartimento di Biologia e Patologia Cellulare e Molecolare “L. Califano”
Università degli Studi di Napoli Federico II

Partner Institutions

Italian Institutions
Università degli Studi di Napoli “Federico II”, Naples, Italy
Istituto di Endocrinologia ed Oncologia Sperimentale “G. Salvatore”, CNR, Naples, Italy
Seconda Università di Napoli, Naples, Italy
Università del Sannio, Benevento, Italy
Università di Genova, Genoa, Italy
Università di Padova, Padua, Italy

Foreign Institutions
Johns Hopkins School of Medicine, Baltimore, MD, USA
Johns Hopkins Krieger School of Arts and Sciences, Baltimore, MD, USA
National Institutes of Health, Bethesda, MD, USA
Ohio State University, Columbus, OH, USA
Université Paris Sud XI, Paris, France
Universidad Autonoma de Madrid, Spain
Centro de Investigaciones Oncologicas (CNIO), Spain
Universidade Federal de Sao Paulo, Brazil
Albert Einstein College of Medicine of Yeshiwa University, USA

Supporting Institutions
Università degli Studi di Napoli “Federico II”, Naples, Italy
Ministero dell’Università e della Ricerca
Istituto Superiore di Oncologia (ISO)
Terry Fox Foundation, Canada
Istituto di Endocrinologia ed Oncologia Sperimentale “G. Salvatore”, CNR, Naples, Italy
Centro Regionale di Competenza in Genomica (GEAR)
Università Italo-Francese

Faculty

Italian Faculty

Giancarlo Vecchio, MD, Co-ordinator
Francesco Beguinot, MD
Angelo Raffaele Bianco, MD
Francesca Carlomagno, MD
Gabriella Castoria, MD
Angela Celetti, MD
Vincenzo Ciminale, MD
Annamaria Cirafici, PhD
Annamaria Colao, MD
Alma Contegiacomo, MD
Sabino De Placido, MD
Monica Fedele, PhD
Pietro Formisano, MD
Alfredo Fusco, MD
Massimo Imbriaco, MD
Paolo Laccetti, MD
Antonio Leonardi, MD
Barbara Majello, PhD
Rosa Marina Melillo, MD
Claudia Miele, PhD
Francesco Oriente, MD
Roberto Pacelli, MD
Giuseppe Palumbo, PhD
Silvio Parodi, MD
Giuseppe Portella, MD
Giorgio Punzo, MD
Antonio Rosato, MD
Massimo Santoro, MD
Giampaolo Tortora, MD
Donatella Tramontano, PhD
Giancarlo Troncone, MD
Bianca Maria Veneziani, MD

Foreign Faculty

National Institutes of Health (USA)
Michael M. Gottesman, MD
Silvio Gutkind, PhD
Stephen Marx, MD
Ira Pastan, MD
Phill Gorden, MD

Johns Hopkins School of Medicine (USA)
Vincenzo Casolaro, MD
Pierre Coulombe, PhD
James G. Herman MD
Robert Schleimer, PhD

Johns Hopkins Krieger School of Arts and Sciences (USA)
Eaton E. Lattman, MD

Ohio State University, Columbus (USA)
Carlo M. Croce, MD

Albert Einstein College of Medicine of Yeshiwa University (USA)
Luciano D'Adamio, MD
Nancy Carrasco, MD

Université Paris Sud XI (France)
Martin Schlumberger, MD
Jean Michel Bidart, MD

Universidad Autonoma de Madrid (Spain)
Juan Bernal, MD, PhD
Pilar Santisteban

Centro de Investigaciones Oncologicas (Spain)
Mariano Barbacid, MD

Universidade Federal de Sao Paulo (Brazil)
Janete Maria Cerutti
Rui Maciel

“Analysis of oncolytic adenovirus *dl*922-947 effects on anaplastic thyroid carcinoma cells (ATC) and potential therapeutic associations”

TABLE OF CONTENTS

LIST OF PUBLICATIONS

This dissertation is based upon the following publication:

- Silvana Libertini, Irma Iacuzzo, Angelo Ferraro, Mario Vitale, Maurizio Bifulco, Alfredo Fusco, Giuseppe Portella. **Lovastatin enhances the replication of the oncolytic adenovirus *dl*1520 and its antineoplastic activity against anaplastic thyroid carcinoma cells.** Endocrinology 2007, 148(11): 5186–5194

ABSTRACT

Anaplastic thyroid carcinoma (ATC) represents one of the most lethal human neoplasia with a survival time of 2-6 months after diagnosis and it is refractory to current available therapies such as chemo- and radiotherapy.
For this reason it is necessary to find new therapeutic approaches and the use of oncolytic viruses represents a promising strategy.
In this study I have evaluated a therapeutic approach based on *dl*922-947, an oncolytic adenovirus bearing a deletion of 24 bp in E1A-Conserved Region 2 (CR2). This adenoviral mutant is unable to bind the product of Rb gene therefore replicates only in neoplastic cells without an intact G1-S checkpoint. This checkpoint is lost in almost all human neoplasias and also in anaplastic thyroid carcinoma. Here I have reported that *dl*922-947 induces cell death in a panel of human anaplastic thyroid cell lines and the *in vivo* experiments, against ATC tumour xenografts, show an improved response rates compared with the adenoviruses *dl*1520. I have also demonstrated that *dl*922/947 has a higher replication efficiency compared with the adenoviruses *dl*1520.
To enhance the antineoplastic effects of *dl*922-947, I have evaluated the effects of a combined treatment with an anti VEGF monoclonal antibody (Bevacizumab) and *dl*922-947 against ATC tumour xenografts. I have observed a significant reduction of tumour growth with respect to single treatments. Furthermore I have observed that the combined treatment enhances the viral distribution within the tumour mass and increases the viral replication. These results suggest that *dl*922-947 may be a valid tool in the treatment of the anaplastic thyroid carcinoma and the combined treatment *dl*922-947/Bevacizumab could represent a novel strategy to improve the delivery of oncolytic viruses into the tumours.

1. INTRODUCTION

1.1 Oncolytic viruses in the treatment of cancer

The notion that viruses may be able to eradicate cancer has existed since the early 20th century (Sinkovics and Horvath 1993, Sinkovics and Horvath 2000, Southam and Moore 1952). Several viruses were tested both in experimental settings and in humans during the 1950s and 1960s. Among the first viruses to be used in a controlled fashion in clinical studies was a vaccine strain of rabies virus to treat 30 patients with melanomatosis, eight of whom showed tumour regression (Pack 1950). A few years later the oncolytic efficacy of adenovirus serotype type 4, was tested in humans (Southam CM et al. 1956), as well as the flavivirus West Nile virus (strain Egypt 101) (Southam and Moore 1952) and the paramyxoviruses mumps and Newcastle disease virus (NDV) (Asada 1974, Okuno et al. 1978). Also, many viruses were tested in animal models. For instance, bovine enterovirus showed efficient lysis of syngeneic tumours in immunocompetent mice (Taylor et al. 1971). Unfortunately all these approaches failed because of an insufficient knowledge about purification systems. Later in the 1990s, with the advent of modern biotechnology and the concept of gene therapy, interest in viruses as a treatment for cancer was rekindled, and today virotherapy is asserting itself as a formidable treatment option alongside surgery, chemo- and radiation therapy.

There are many reasons that can explain the use of viruses in cancer therapy, in particular cancer cells are generous hosts for viruses, being preferred over other types of cells because of they may simultaneously lose critical components of the intracellular defence mechanisms and thus become fertile ground for the replication of many viruses. Oncolytic viruses are able to replicate only in cancer cells but not in normal cells and being mutated to be dependent on certain molecular defects in cancer cells they are called conditionally replicating (i.e. restricted to replicate only in permissive cells). For example, some adenoviral vectors have been deleted for the E1B gene in order to restrict their replication to cells in which the function of the p53 protein is impaired. As another example, herpes viruses lose the ability to infect non-dividing cells by deletion of the thymidine kinase gene, thereby forcing these viruses to prefer tumour cells over normal cells (Martuza 1991).

Members from an increasing number of virus families are being considered for cancer gene therapy. Some of these viruses are reported in table below (table 1). In the following some further details will be given only about the ones used in clinical trials.

Table 1: Oncolytic virus in cancer gene therapy

Virus	Phase of development
Herpes Simplex Virus	Phase I in glioma patients
Poliomavirus	Tested in preclinical models
Poxvirus	Phase I in refractory and/or current melanoma patients
Reovirus	Phase I in glioma and melanoma patients
Newcastle disease virus	Phase I in advanced solid cancer patients
Rhabdovirus	Tested in preclinical models
Coronavirus	Tested in preclinical models
Picornavirus	Tested in preclinical models
Retrovirus	Tested in preclinical models
Adenovirus	Phase I/II/III

In this table a group of the most important oncolytic viruses is reported. Oncolytic viruses that are used in different phase of clinical trials are indicated in blue.

1.1.1 Herpes simplex virus

HSV-1 is an enveloped, double-stranded DNA virus with a genome size of approximately 152 kb. There are two general strategies that are employed to target HSV-1 replication to cancer cells. The first involves deletion or inactivation of viral genes that are essential for viral replication in normal cells but dispensable in tumour cells, such as HSV-tk, ribonucleotide reductase, and γ134.5. The initial HSV-1 mutant studied for tumour-selective replication, *dl*sptk, contains a 360-bp deletion within HSV-tk, and it was used to treat malignant gliomas in rodents (Martuza 1991). Accordingly, *dl*sptk replicates well in cultured tumour cells and induces significant growth inhibition of human U87 gliomas growing in the brains of nude mice. However, this HSV-1 mutant has not been examined in clinical trials because it produces neurotoxicity at higher titers, and it is resistant to the antiviral agents acyclovir and ganciclovir by virtue of its disrupted HSV-tk gene. Investigators looked instead at developing HSV-1 mutants that maintain sensitivity to acyclovir and ganciclovir and that exhibit less neurovirulence by deletion of the γ134.5 gene. One such γ134.5-null mutant is G207 (MediGene, Inc.; San Diego, CA) which exhibits tumour-cell-specific replication and antitumour efficacy in both *in*

vitro and *in vivo* models of malignant glioma (Mineta 1995) and a study of a phase I was conducted in patients with glioma (Shah 2003).

1.1.2 Poxvirus

Poxviruses are large, enveloped, dsDNA viruses with a complex genome harbouring multiple immune-modulating genes. The most commonly used poxvirus in cancer targeting is vaccinia virus (VV). Vaccinia virus has tropism for human cells and its high immunogenicity. Three properties of vaccinia virus are being used to develop the virus as a cancer therapy: (1) vaccinia virus has a high efficiency of infection, it replicates in the cytoplasm without chromosomal integration, and the 200 kb genome allows the insertion of a large amount of recombinant DNA without losing infectivity; (2) to develop cancer vaccines, the immunostimulatory properties of the virus are being harnessed to incite an immune response against cancer cells; (3) to develop an oncolytic virus, replication conditional viral mutants are being constructed to target specific cancer types. Vaccina virus was used in preclinical and phase I trials. Wild-type vaccinia virus does not selectively infect cancer cells. The virus requires modification to be made replication conditional. One strategy is to delete the viral TK gene. While the viral TK gene is necessary for infectivity in normal cells that possess small concentrations of intracellular nucleotide pools, it is not necessary in cancer cells (Mastrangelo 1999) which possess relatively high concentrations of intracellular nucleotides. Another novel vector involved replacing the viral TK gene with the gene for GM-CSF, creating a mutant vaccinia virus capable of selectively infecting melanoma cells, and inducing an antitumour immune response. This virus has been administered intralesionally in a phase I clinical trial involving patients with refractory and/or recurrent melanoma. Injected lesions contained an active inflammatory response and demonstrable viral replication (Mastrangelo 1999).

1.1.3 Reovirus

Reovirus is a ubiquitous, nonenveloped double-stranded RNA virus with minimal pathogenicity in humans. Infections in humans are generally mild and restricted to the respiratory and gastrointestinal tracts. It was known that reovirus exhibited preferential cytotoxicity for transformed cells compared with normal cells (Hashiro et al. 1977, Duncan et al. 1978). Given the facts that reovirus exhibits preferential replication in cells with an activated *ras* signalling pathway and that some 30% or more of all human tumours possess an activating mutation of *ras*, reovirus appears to be an ideal oncolytic agent. Coffey et al. (1998) examined the efficacy of reovirus against flank tumours

established from v-*erbB*-transformed NIH 3T3 cells and human U87 glioblastoma cells, which overexpress the platelet-derived growth factor receptor and thus have an activated *ras* pathway. A single intratumoural injection of 1×10^7 plaque forming units (pfu) of reovirus resulted in tumour regression in 65%-80% of mice. The virus also proved effective in treatment of tumours established from *ras*-transformed C3H-10T1/2 cells in immunocompetent C3H mice, and pre-existing immunity to reovirus did not abrogate the oncolytic effect. More recently, data were presented that intravenous administration of reovirus is effective in reducing tumour burden and prolonging survival of mice bearing Lewis lung carcinoma metastases (Hirasawa 2001) and a study of a phase I was conducted in patients with glioma and melanoma.

1.1.4 Newcastle disease virus

NDV is a chicken paramyxovirus and an enveloped negative-stranded RNA virus. The virus is not pathogenic to humans and has been extensively studied as an oncolytic agent in several different human tumour cell lines and tumour models (Reichard 1992 and Lorence 1994). The first report of activity with Newcastle virus involved one patient with cervical cancer. Cassel and Garrett (1965) injected virus (2.4×10^{12} virus particles) directly into the tumour and demonstrated intratumoural regression of the cancer both at the injection site and at a distant malignant lymph node. Investigators at Pro-Virus, Inc. (Gaithersburg, MD) have isolated a naturally attenuated strain of NDV, cloned by nonrecombinant methods, that exhibits a broad range of oncolytic activity against human tumours. This strain, designated PV701, is characterized by its *in vitro* potency, as a ratio of 1 pfu to 10,000 tumour cells results in at least 50% lysis of sensitive tumour cell lines in 5 days. PV701 is also characterized by its tumour selectivity, as 80% of human cancer cell lines are two to four log orders more sensitive than normal human cells to PV701-mediated killing (Roberts et al. 2001). These encouraging preclinical data have led to the initiation of a phase I clinical trial of PV701 administered intravenously to patients with advanced solid cancers who failed conventional therapy (Pecora et al. 2002).

1.1.5 Adenovirus

Adenoviruses are the most widely used oncolytic viruses in cancer therapy and also the most widely described, moreover there is a great number of clinical trials in which these viruses are used.

a) Biology of adenovirus

Adenovirus is a non-enveloped, 80-110 nm diameter virus presenting icosahedral symmetry. The 51 distinct serotypes of human adenovirus have been classified into six groups (A–F) based on sequence homology and their ability to agglutinate red blood cells (Shenk 1996). Most studies have been carried out on adenovirus serotype 2 (Ad2) and Ad5. Human adenoviruses contain a linear, double stranded DNA genome of 30-36 Kb. The hexon, penton base, and knobbed fiber, are the most important capsid proteins for gene delivery. Adenovirus infection occurs through binding of the adenoviral fiber to cellular receptors such as the coxsackie-adenovirus receptor (CAR) or integrins (Fig.1).

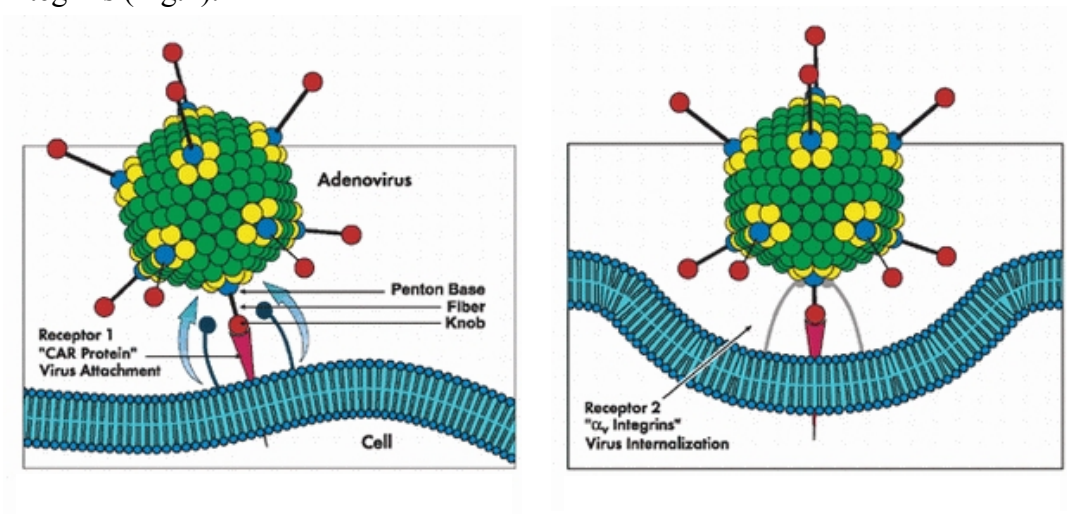

Figure 1: Adsorption and entry of adenovirus into the cell
Attachment of adenovirus to cell surface receptor (on the left) and receptor-mediated endocytosis (on the right).

After the virus internalization through endocytosis the virus escapes the endosome and translocates to the nuclear pore complex, where the viral DNA is released into the nucleus and transcription begins. Transcription, replication and viral packaging take place in the nucleus of the infected cell. A complex series of splicing accompanies transcription, and genes are transcribed from both strands. Adenoviral transcription occurs in two phases: early and late (Fields et al. 1996) (Fig.2).

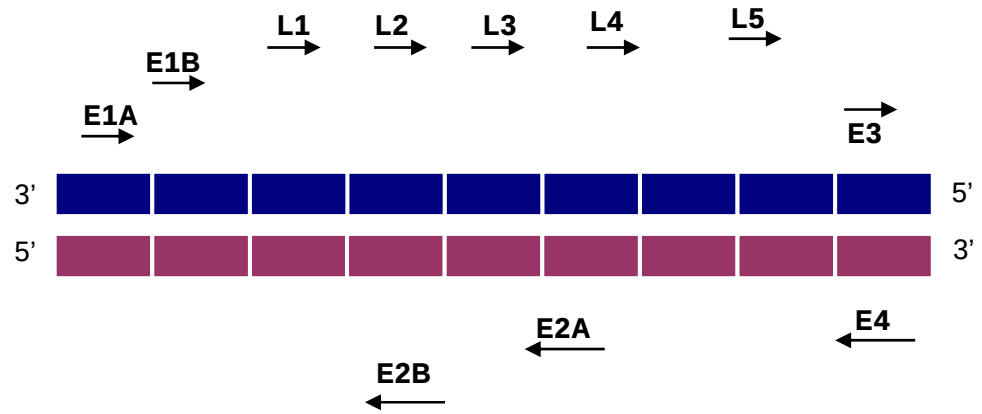

Figure 2: Adenoviral genome
The early and late gene of viral life-cycle are represented

During the early phase, the host cell is transformed into an efficient producer of the viral genome. The first gene that is transcribed in the viral genome is *E1A*. The adenovirus E1A protein is encoded by several alternatively spliced mRNAs, with the predominant forms being the 12S and 13S mRNAs (Heise et al. 2000). Two regions of conserved sequence among E1A proteins of different adenovirus types are conserved regions 1 and 2 (CR1 and CR2). CR1 and CR2 contribute to E1A-induced cell cycle progression and transformation (Fueyo et al. 2000, Rodriguez et al. 1997). During infection, the primary mechanism by which E1A forces quiescent cells to actively cycle is by interfering with proteins of the retinoblastoma (Rb) pathway (Harlow et al. 1986, Moran 1993) and this interaction is mediated primarily by CR2. Rb acts as a tumour suppressor via binding to E2F, a transcriptional activator that promotes expression of genes necessary for driving the cell into S phase (Nevins 1995). The E1A product is able to sequester Rb and release repression of E2F, allowing it to activate its target genes. E1A proteins have also been shown to modulate the activity of p107 and p130, two members of the Rb family that are also involved in regulating cell cycle progression (Parreno et al. 2001). In addition to binding to Rb, E1A also binds to p300, an important nuclear integrator of diverse signalling pathways that possesses intrinsic histone acetyltransferase (HAT) activity and is implicated in the activation of genes that maintain cell differentiation and inhibit the cell cycle. p300 regulates and activates transcription by acetylating multiple other transcription factors, E2F and p53 being two important examples. E1A has been shown to repress directly the HAT activity of p300 and to inhibit p300-dependent transcription (Hamamori et al. 1999, Chakravarti et al. 1999). All these actions of E1A result in the accumulation of p53. p53 is a cellular growth suppressor that acts as a G1 checkpoint control and in response to viral challenge, p53 may induce a G1 growth arrest by inducing genes such as the cyclin-dependent kinase inhibitor p21/WAF1/Cip1 gene (El-Deiry et al. 1993, Xiong et al. 1993) or apoptosis by

inducing genes such as *bax1* (Miyashita and Reed 1995). However the induction of apoptosis is inhibited by the products of the E1B gene. The E1B transcription unit encodes two proteins, E1B-55kDa and E1B-19kDa. The E1B-19kDa protein is a functional homologue of the proto-oncogene-encoded Bcl-2 and prevents apoptosis by similar mechanisms (Debbas et al. 1993, Rao et al. 1992). The E1B-55kDa protein complexes with the amino-terminal end of p53 and inhibits its activity as a transcription factor (Kao et al. 1990, Yew and Berk 1992, Yew et al. 1994). It is thought that these mechanisms for inhibiting apoptosis keep the cell alive as long as possible in order to maximize viral yields (Rao et al., 1992). In addition to its antiapoptotic functions, the E1B-55KDa protein facilitates the transport of viral mRNAs to the cytoplasm during the late stages of infection (Pilder et al., 1986).
The E2 region encodes proteins necessary for replication of the viral genome: DNA polymerase, preterminal protein, and the 72-kDa single-stranded DNA-binding protein (De Jong et al. 2003).
Products of the viral E3 region function to subvert the host immune response and allow persistence of infected cells. The immune system has evolved a number of mechanisms for destroying virus-infected cells, including cell lysis by cytotoxic T lymphocytes and activation of receptor-mediated apoptotic pathways by chemokines.
The E4 transcription unit encodes a number of proteins that have been known to play a role in cell cycle control and regulation of DNA replication.
The viral structural proteins and the proteins necessary for assembly of the virion are encoded by genes expressed during the late phase of viral replication. Once viral progeny assembly is complete, new viral particles are released by cytolysis.

b) Methods to render cytolytic adenoviruses tumour specific

There are different ways in order to developing tumour specificity in oncolytic adenoviruses:
- by placing viral genes that initiate viral replication under the control of promoter sequences that are active only in tumour cells
- by the modification of viral coat proteins that function in host cell infection.
- by altering viral genes that attenuate replication in normal tissue but not in tumour cells

The first strategy concerns the regulation of viral replication via cellular promoters that are overactive in certain tumour cells, sometimes referred to as "tumour-specific" promoters (Fig.3). Certain tumour types, such as germ cell tumours, prostate cancer, and hepatocellular carcinoma, express proteins that are not normally present in the human body after fetal development. Certain oncolytic adenoviruses have been created to take advantage of the expression of these tumour markers or dependence on normally secreted hormones by placing the *E1A* gene under the control of the promoters derived from the

genes of interest. The oncolytic adenovirus AvE2a04i (Hallenbeck et al. 1999), was created to target α-fetoprotein (AFP)-expressing hepatocellular carcinoma by placing *E1A* under the control of the *AFP* gene promoter. CV706 targets prostate cancer by placing *E1A* under the control of a promoter derived from the prostate-specific antigen (*PSA*) gene (Rodriguez et al. 1997). AdhOC-E1 targets prostate tumour cells by using a promoter derived from the *osteocalcin* gene (Matsubara et al. 2001, Hsieh et al. 2002), the product of which is also secreted by prostate tumour cells. One major limitation with the use of these tumour-activated promoters to regulate adenovirus replication is that they are not always active in all tumour types. In fact the transcriptional activity for the driving promoter must be conserved in the target tumour, therefore promoter driven oncolytic adenoviruses are often not active against poorly differentiate carcinomas.

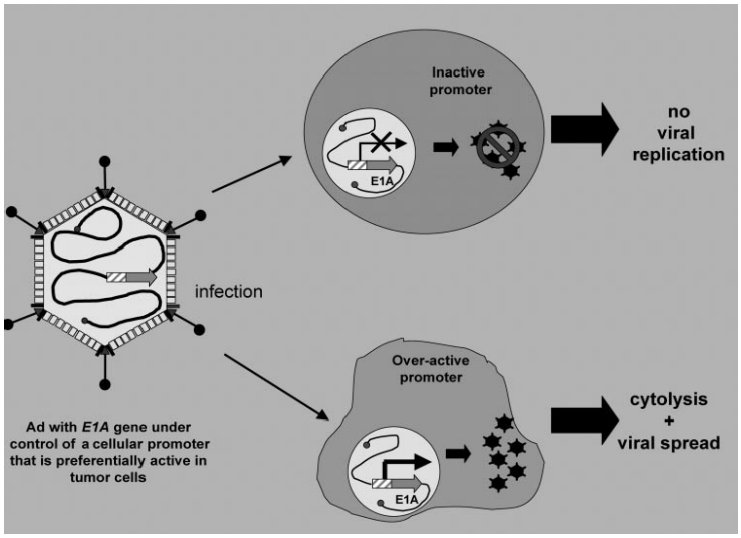

Figure 3: Use of cellular promoters to direct lytic viral replication to tumour cells
The *E1A* gene (*gray arrow*) is placed under control of a promoter (*dashed rectangle*) that is preferentially overactive in a given tumour cell-type. This modification drives viral replication in tumour cells but not normal cells.

The second strategy used to create oncolytic adenovirus is to alter the structural viral envelope proteins to retarget the virus to tumour cell surfaces and direct the virus away from its normal receptor (Fig.4). The attachment of adenoviruses to a cell is initiated by interaction of the knob domain of the viral fiber protein with cell surface proteins such as the coxsackie-adenovirus receptor (Bergelson et al. 1997, Tomko et al. 1997). After attachment, the Arg-Gly-Asp (RGD) peptide sequence within the viral penton protein interacts with αvβ3 and αvβ5 integrins, which then leads to the internalization of the virus by receptor-mediated endocytosis. One modification is to incorporate the RGD

motif into the knob protein that normally binds to the CAR. By adding this motif to the knob protein, the oncolytic adenovirus can infect a broader range of tumour cells, because αvβ3/5 integrins are expressed on a majority of cells. Another strategy consists in fusion between ectodomain of CAR and epidermal growth factor in order to mediate adenovirus targeting to epidermal growth factor receptor-positive cells (Dmitriev et al. 2000).

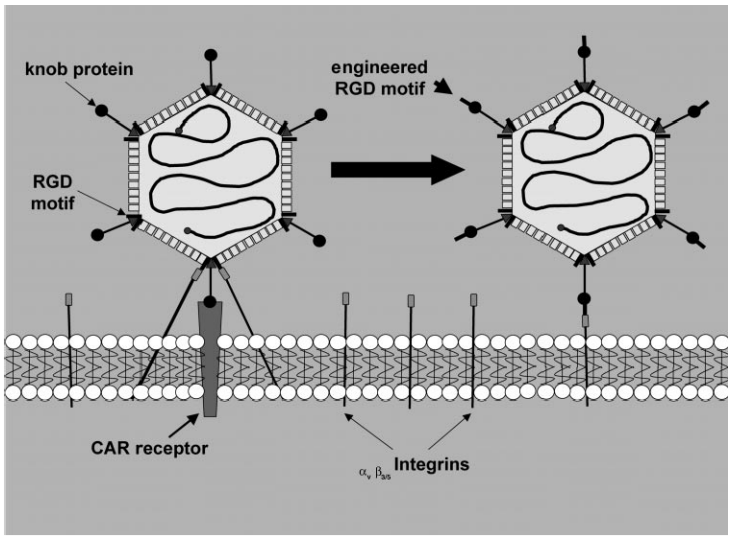

Figure 4: Targeting viral infection to tumour cells through alterations in viral-host cell interactions
One modification is to incorporate the RGD motif into the knob protein that normally binds to the CAR (see extension on knob circle in virus on right). By adding this motif to the knob protein, the oncolytic adenovirus can infect a broader range of tumour cells, because αvβ3/5 integrins are expressed on a majority of cells.

The last and the most widely-used strategy consists in the creation of replication-conditional adenoviruses genetically modified such as *dl*1520 and *dl*922-947.
Mutant adenovirus *dl*1520 (also known as ONYX-015) contains a deletion in the *E1B* gene, preventing the formation of a functional E1B-55kD protein. With this mutation, *dl*1520 was expected to replicate only in p53-deficient cells (Bischoff et al. 1996). (Fig. 5).

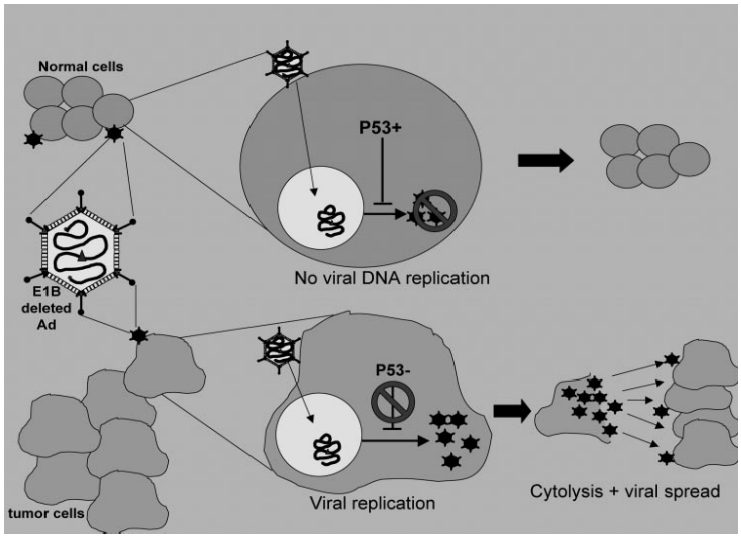

Figure 5: Attenuating viral replication in normal cells but not tumour cells via gene mutation.
For example, by altering a region of the *E1B* gene, the adenovirus can selectively replicate in p53-deficient (*i.e.* tumour) cells and leave p53- competent cells intact.

However, more recent studies show that *dl*1520 was able to replicate in cells with a wild-type *TP53* gene (Gallimore and Turnell 2001, Petit et al. 2002, Geoerger et al. 2002, Harada and Berk 1999, Rothmann et al. 1998, Hall et al. 1998, Goodrum and Ornelles 1998). There are several explanations for these conflicting results. There are other proteins that affect p53 activity in cells, such as p14ARF and mdm2 (Bischoff et al. 1996, Yang et al. 2001, Ries et al. 2000). p14ARF down-regulates mdm2, which is an ubiquitin ligase that stimulates p53 degradation. Cancer cells with a loss in *p14ARF* gene expression due to gene deletion or with overexpression of mdm2 after gene amplification will create a p53-null phenotype thereby allowing *dl*1520 replication in tumours containing a wild-type *TP53* gene. Another explanation involves the adenoviral *E4orf6* gene product, which also binds to p53 and inhibits p53-mediated apoptosis, possibly allowing E1B-55kDa-deficient adenoviruses to replicate in cells with wild-type p53 (Aoyagi et al. 2003). In addition to its role in the degradation of p53, the E1B-55kDa protein has several other important late-phase functions. For example, E1B-55KDa mediates late-viral RNA transport and the loss of E1B-55KDa restricts the viral replication to tumour cells capable of taking over the RNA export function of the viral gene product (O'Shea et al. 2005).
*dl*1520 has been used in conjunction with chemotherapeutic agents in clinical trials of a phase I/II with evidence for potential synergistic antitumour activity. (Post et al. 2003). And recent results from a phase III clinical trial have confirmed the ability of an oncolytic adenovirus (H101) bearing a E1B-55kDa gene deletion similar to that present in *dl*1520, to increase the response rate of

nasopharyngeal carcinoma in combination with cisplatin (Crompton and Kirn 2007, Yu and Fang 2007).
A second generation adenoviral mutant is *dl*922-947, which is an E1A mutant. *dl*922–947 has a 24-bp deletion in E1A Conserved Region 2 (CR2) therefore, is unable to induce progression from G1 into S-phase of quiescent cells. The G1-S checkpoint is critical for cell growth progression and is lost in almost all cancer cells as a result of mutations or deletions of the RB or *CDKN2A* genes, amplification and overexpression of Cyclin D, and amplification, overexpression or mutation of the CDK4 gene (Sherr 2000, Roussel 1999). The *in vitro* efficacy of *dl*922-947 was demonstrated in a range of a cancer cell lines and this efficacy exceeded that of adenovirus 5 wild-type (Ad5wt) and *dl*1520 (Heise et al. 2000). A similar adenovirus, Δ24, with the same deletion in E1A-CR2, has shown activity in preclinical models of glioma (Fueyo et al. 2000). *dl*922-947 has also an impressive in vitro activity in ovarian carcinoma and was able to produce some long-term survivors in an aggressive xenograft model (Lockley et al. 2006).

c) Oncolytic adenoviruses in combination cancer therapies

The safety and antitumour efficacy of *dl*1520 alone have been tested in numerous phase I and II clinical trials (Kirn 2001). In all cases safety was demonstrated, with the most common associated toxicity being flulike symptoms. Some of the most encouraging data were obtained from a phase II study using intratumoural administration of *dl*1520 in patients with advanced head and neck squamous cell carcinoma (Nemunaitis et al. 2000, 2001b). In all this trials adenovirus was administered alone and this mono-therapy has demonstrated limitations in efficacy. The best chance for complete tumour eradication lies in a multimodal cancer therapy approach utilizing oncolytic viruses in conjunction with chemotherapy and radiotherapy. The rationale for combination therapy was that a greater antitumour effect was expected with combination treatment compared with single therapies; the therapies have different toxicity profiles and may result in enhanced efficacy without increased adverse events; no overlapping resistance between oncolytic viruses and chemotherapy and radiotherapy was anticipated; and it may be possible to lower treatment doses, thereby decreasing treatment cost, with combination therapy and still achieve a greater therapeutic efficacy than with single-modality treatment. *dl*1520 has been used in conjunction with chemotherapeutic agents in clinical trials with evidence for potential synergistic antitumour activity. The use of *dl*1520 in conjunction with cisplatin (causes intrastrand DNA cross-links that block DNA replication), and 5-fluorouracil (pyrimidine antagonist that inhibits DNA synthesis) has been examined in a phase II clinical trial involving head and neck carcinoma patients. *dl*1520 has been used in combination with leucovorin and 5-fluorouracil in a phase II trial in patients with gastrointestinal carcinoma

metastatic to the liver and with gemcitabine in a phase I/II trial in patients with unresectable pancreatic carcinoma (Kruyt and Curiel 2002, Post et al. 2003). A variant of *dl*1520, H101, an E1B-55KDa-deleted adenovirus, was tested in a phase III study. In this trial the adenovirus was given by intratumoural injection to patients who received cisplatin-based chemotherapy. In studies of patients with squamous cell cancer of the head and neck or of the oesophagus, the response rate was significantly higher (78%) in patients who received the combination of viral therapy and chemotherapy than in patients who were treated with chemotherapy alone (39%) (Xia et al. 2004, Wakimoto et al. 2004).

All these studies have shown that combined treatment *dl*1520-chemotherapy increases the therapeutic effects. There have been several theories proposed for the augmented therapeutic effects of combined oncolytic adenoviruses and chemotherapy and the mainly one is that chemotherapy may enhance virus replication.

Radiation has also been shown to be effective in combination with oncolytic virotherapy. Radiation therapy-induced tumour cell death is dependent on directly damaging DNA or indirectly through the formation of oxygen radicals that disrupt cellular pathways. This dual mechanism is different from how oncolytic viruses destroy tumour cells. This has led to several preclinical trials looking at the role of combining these two modalities. Intra-arterial injections of *dl*1520 in conjunction with total body irradiation (5 Gy) were evaluated in subcutaneous human malignant glioma xenograft models that were either p53 mutant or p53 wild-type (Geoerger et al. 2003). Significant tumour growth delays were noted in the p53 mutant tumours receiving combination therapy *versus* monotherapies (30 days *versus* 10–15 days). The combination of low doses of *dl*1520 with a single 10 Gy dose of radiation significantly delayed the growth of xenograft tumours induced in athymic mice by the injection of anaplastic thyroid carcinoma cell lines (Portella et al. 2003). Qian et al. (2005) have observed an increase of viral uptake in irradiated cells, and suggested a crucial role for a protein involved in adenovirus endocytosis, Dynamin 2. In summary, these preclinical studies in combining oncolytic adenoviruses with radiation therapy provided several important findings. Radiation did not appear to impair viral replication (Rogulski et al. 20001, Geoerger et al. 2003, Lamfers et al. 2002, Chen et al. 2001). There also appears to be no additive toxicities noted in the virus plus radiation-treated groups compared with the monotherapy groups (Rogulski et al. 2000, Chen et al. 2001). Furthermore, these preclinical studies point to enhanced antitumour effects when compared with monotherapy. Another interesting finding is, like in combination with chemotherapy, the order in which oncolytic adenoviral therapy and radiation therapy are administered may be important.

*dl*1520 appears to be a good candidate also in combination with gene therapy and for this reason a new therapeutic strategy, called “targeting gene-virotherapy”, is proposed. Basically, the antitumour gene is inserted into the tumour-specific replicative viral vector which then delivers the antitumour

gene to the tumour cells. There are many ways to construct tumour-specific replicative viral vectors. It was constructed the modified adenoviral vector pZD55, with E1B55KDa deleted, but E1A remained, which specifically targeted p53-deficient tumour cells. The recombinant adenovirus was named ZD55, and it is similar to ONYX-015, but it is Ad5, not Ad2/Ad5 fusion virus, and furthermore there is a cloning site in ZD55 which is convenient to insert an exogenous gene into it (Zhang et al. 2003). Another way to construct tumour-specific replicative viral vectors is to introduce a tumour-specific promoter to control the essential elements of viral replication, such as E1A and E1B. Therefore, these viruses and the inserted antitumour genes can only be replicated and expressed in tumour cells (Chiocca 2002). Many tissue-specific promoters are available for constructing tumour cell-specific replicative adenoviruses, such as AFP promoter for hepatic cancer, PSA promoter for prostate cancer, MUC-1 promoter for breast cancer and hTERT promoter.

1.2 Angiogenesis is a novel therapeutic target for cancer treatment

One of the major obstacle to the successful application of therapeutic strategies based on replicating oncolytic viruses is represented by the poor distribution of viral particles throughout the tumour mass. This insufficient distribution is due to many causes among which there are physical barriers. In fact viruses delivered via the vasculature must cross the blood vessel endothelium and any layer of matrix that separate the endothelial cells from the tumour represent an obstacle for viral dissemination. Also host-derived connective tissue, including components of the basement membrane and the extracellular matrix (ECM), acts as a passive barrier to viral spread. In addition to the physical barriers solid tumours contain physiologically different sub-compartments which may influence virus entry, diffusion and half-life. For example, in areas of necrosis or calcification, common to growing tumour masses *in vivo*, the prevailing microenvironment is characterized by hypoxia, acidosis and enhanced proteolytic activity, which may affect the virus particle itself or modify the cell surface of nearby live tumour cells in an unfavorable manner (Cairns et al. 2006).

Moreover, tumour vessels are structurally and functionally abnormal. In contrast to normal vessels, tumour vasculature is highly disorganized, vessels are tortuous and dilated, with uneven diameter, excessive branching and shunts (Fig. 6).

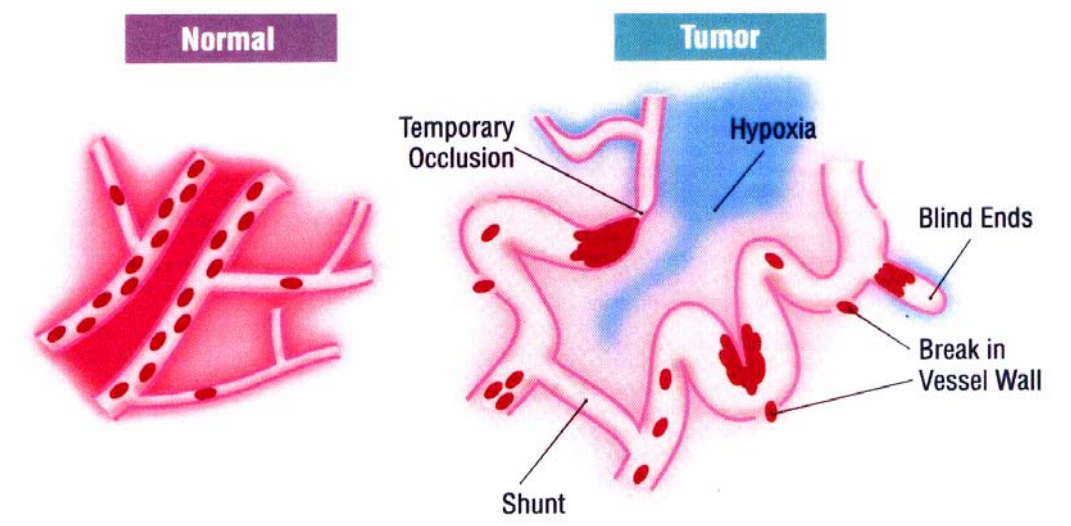

Figure 6: Abnormal tumour vessels
Tumour vessels are disorganized with shunts, occlusions, blind ends and breaks in vessel walls

This may be due to an imbalance of angiogenic regulators, such as vascular endothelial growth factor (VEGF) and angiopoietins. Consequently, tumour blood flow is chaotic and variable (Baish and Jain 2000). In terms of their ultra structure, tumour vessels are also abnormal: their walls have numerous 'openings' (endothelial fenestrae, vesicles and transcellular holes), widened interendothelial junctions, and a discontinuous or absent basement membrane. In addition, the endothelial cells are abnormal in shape, growing on top of each other and projecting into the lumen and, as a result of vascular hyperpermeability, tumour vessels are unable to maintain gradients between vascular and interstitial pressures, which contributes to interstitial hypertension. This lack of pressure gradient also impairs the flow of fluids, macromolecules and therapeutic agents. All these pathophysiological characteristics of solid tumours compromise the delivery and effectiveness of conventional cytotoxic therapies as well as molecular targeted therapies.
Recently, a number of strategies to enhance the delivery of viruses into solid tumours have been proposed (McKee et al. 2006, Cairns et al. 2006, Minchinton and Tannock 2006). For example, given the physical barriers to oncolytic viruses, pre-treatment with proteolytic enzymes, e.g. hyalorunidase or collagenase, could alter the ECM and thus facilitate virus penetration. Therefore I have decided to evaluate the effects of a combined treatment between the oncolytic adenovirus *dl*922-947 and Bevacizumab, a recombinant humanized monoclonal antibody to the VEGF.
Bevacizumab, has been tested in the clinic and has shown promising results (Ferrara et al. 2004, Gordon et al. 2001, Yang et al. 2003). Additionally, when combined with chemotherapy or radiotherapy, Bevacizumab has shown additive to synergistic effects on tumour inhibition (Ferrara et al. 2004, Hurwitz et al. 2004, Gerber and Ferrara 2005). A recent study on preclinical

model demonstrated that inhibition of carcinoma cell-derived VEGF by Bevacizumab reduced macrophage infiltration and activity, angiogenesis, vascular leakage, extracellular fluid volume in KAT-4 tumours (Salnikov et al. 2006). Moreover Ad-mda7, a recombinant adenoviral vector of melanoma differentiation associated gene-7, with a potent antitumour and antiangiogenic activity both *in vitro* and *in vivo,* in combination with Bevacizumab treatment produces a synergistic and complete inhibitory effect on lung tumour xenografts.

2. AIMS OF THE STUDY

Thyroid carcinoma accounts for roughly 1% of all new malignant disease. Of these, at least 94% are differentiated thyroid carcinomas that derive from the follicular epithelial cells; and are either papillary thyroid carcinoma or follicular thyroid carcinoma. Another 5% are medullary thyroid carcinoma, a neuroendocrine tumour and the remaining 1% are anaplastic thyroid carcinoma that generally derive from dedifferentiation of the differentiated type.

Anaplastic thyroid carcinoma is associated with a disease-specific mortality of almost 100% (Pierie et al. 2002, Xu et al. 2001, McIver et al. 2001, Haigh et al. 2001, Passler et al. 1999, Hundahl et al. 1998). Patients with anaplastic carcinoma usually present with widespread local invasion and a high frequency of distant metastases (Sherman 1999). Treatment of anaplastic-type carcinoma is generally palliative in its intent for a disease that is rarely cured and almost always fatal. The median survival from diagnosis ranges from 3 to 7 months. Therefore, is important to find new therapeutic strategies and oncolytic viruses seem to be a good candidate. The first replication-competent adenoviral mutant described was *dl*1520 and in it was previously demonstrated that *dl*1520 is active against ATC cell lines and tumour xenografts, however high multiplicity of infections (MOIs) of *dl*1520 were used (Portella et al. 2002). This limited efficacy observed against ATC cells highlights a need for oncolytic adenoviruses with higher replication efficiency and killing activity.

In this study I want to evaluate a therapeutic approach of anaplastic thyroid carcinoma based on the use of a second-generation adenoviral mutant, *dl*922-947. This adenovirus lacks in Conserved Region 2 of E1A gene and is able to replicate in cells with an altered G1-S checkpoint. I want to demonstrate that *dl*922-947 has a higher efficiency to kill a range of human anaplastic thyroid cell lines respect to *dl*1520. One of the major obstacle to the successful application of therapeutic strategies based on replicating oncolytic viruses is represented by the poor distribution of viral particles throughout the tumour mass. This is the consequence of a compromised vascular supply with necrotic areas, a distorted functional properties of tumour vessels and a elevated tumour interstitial fluid pressure. In order to improve the delivery of the virus into the tumour, I want to apply a strategy based on the use of Bevacizumab a monoclonal antibody against VEGF. I want to demonstrate that administration of Bevacizumab increases the uptake of *dl*922-947 and that the combined treatment Bevacizumab/*dl*922-947 significantly improves the effects *dl*922-947 against ATC tumour xenografts.

3. MATERIALS AND METHODS

3.1 Cell lines

The human anaplastic thyroid carcinoma cell lines used in the study are ARO, FRO, KAT-4, Cal 62 and BHT-101. ARO and FRO human thyroid anaplastic carcinoma cell lines were obtained by Dr. Juillard (University of California LA). KAT-4 cell line was established by dr. Ain (University of Kentucky, Lexington, KY). Cal 62 cell line was obtained from Deutsche Sammlung von Mikroorganismen und Zellkulturen GmbH (Braunschweig, Germany), German Collection of Microorganisms and Cell Cultures. BHT-101 cell line was established by Dr. Palyi, (National Institute of Oncology, Hungary). The NPA line derives from poorly differentiated papillary carcinoma and was obtained by Dr. G. J. Juillard. The FB1 cell line derives from a follicular carcinoma. Human embryonic kidney HEK-293 cells were obtained from American Type Culture Collection (Manassas, VA).
Cells were grown in DMEM medium supplemented with 10% FCS and ampicillin/streptomycin.

3.2 Preparation of adenoviruses

*dl*1520 (ONYX-015) is a chimaeric human group C adenovirus (Ad2 and Ad5) that has a deletion between nucleotides 2496 and 3323 in the E1B region that encodes the 55- kDa protein. In addition, there is a C to T transition at position 2022 in region E1B that generates a stop codon at the third codon of the protein.
*dl*922-947 is a second generation adenoviral mutant that has a 24-bp deletion in E1A Conserved Region 2 (CR2) therefore, is unable to induce progression from G1 into S-phase of quiescent cells.
AdGFP is a non replicating E1 and E2-deleted adenovirus encoding green fluorescent protein.
Ad5wt is a non-mutant adenovirus used as control adenovirus.
Viral stocks were expanded and titered in the human embryonic kidney cell line HEK-293, which expresses the E1 region. Stocks were stored at -80°C after the addition of glycerol to a concentration of 50% vol/vol. Virus titer was determined by plaque-forming units (pfu) on the HEK-293 cells.

3.3 Viability assay

For the evaluation of the cytotoxic effects of the *dl*922-947 virus, cells were seeded in 96-well plates, and 24 h later increasing concentrations of *dl*922-947, *dl*1520 or control adenovirus Ad5wt were added to the incubation medium. For the evaluation of the cytotoxic effects of the *dl*922-947 virus in combination with paclitaxel, cells were seeded in 96-well plates, and 24 h later were treated

with increasing concentrations of paclitaxel. After 24 h increasing concentrations of *dl*922-947 was added to the incubation medium.
Ten-twelve days later, the media were fixed with 10% TCA and stained with 0.4% sulforhodamine B in 1% acetic acid. The bound dye was solubilized in 100 µl of 10 mM unbuffered Tris HCl solution and the optical density was determined at 540 nm in a microplate reader (Biorad). The percent of survival rates of cells exposed to adenovirus vectors were calculated by assuming the survival rate of untreated cells to be 100%.

3.4 Quantitative PCR of adenoviruses and analysis of adenoviral genes expression

To quantify the amount of viral genomes, cells were infected with *dl*922-947, *dl*1520, and Ad5wt at concentration of 0,1 pfu, 1 pfu and 100 pfu. After 48 h of infection, cell media was collected and viral DNA extracted using a QIAamp DNA mini kit (Valencia, CA, USA) and then quantified by Real-time PCR using assay-specific primer and probe. Real time-based assay was developed using the following primers: 5'-GCC ACC GAG ACG TAC TTC AGC CTG -3' (Upstream primer) and 5'- TTG TAC GAG TAC GCG GTA TCC T- 3' (Downstream primer) for the amplification of 143 bp sequence of the viral hexon gene (from bp 99 to 242 bp). For quantification, a standard curve was constructed by assaying serial dilutions of *dl*1520, *dl*922-947 and Ad5wt viruses ranging from 0,1 pfu to 100 pfu.
To analyze the expression of adenoviral genes ARO and KAT- 4 cells were infected with 10 pfu of *dl*922-947, *dl*1520 and Ad5wt, and harvested at 24 hours post infection. Cells were dissolved in 1 ml Trizol (Invitrogen) and RNA extraction was performed. RNA quality was evaluated by agarose gel electrophoresis, DNAse treatment was performed. 1 µg of total RNA was reverse transcribed using the a SuperScript^{TM} II Reverse Transcriptase Kit (Invitrogen) and the expression of *E1A 13 S* and *Penton* adenoviral genes monitored using Real-time PCR with the following specific primers, *E1A 13 S* Forward: 5'- AAT GGC CGC CAG TCT TTT- 3' and Reverse: 5' - ACA CAG GAC TGT AGA CAA -3'. *Penton* Forward: 5' – TAA CCA GTC ACA GTC GCA AG – 3' and Reverse 5' – CCC GCG CCT TAA ACT TAT T – 3'. As control the expression of β-actin gene was monitored using the following primers: Reverse: 5' – TCG TGC GTG ACA TTA AGG AG – 3' and Forward: 5' – GTC AGG CAG CTC GTA GCT CT – 3'. To calculate the relative expression levels it was used the $2^{-[delta][delta]Ct}$ method. Negative controls, samples without RT PCR or cDNA template were included in every PCR run, always resulting negative (data not shown).

3.5 AdGFP infection

Cells were detached, counted, and plated in 6 well plate at 70% cell density. After 24 h cells were treated with Bevacizumab and then, after 48 h of

incubation, infected with AdGFP, a non replicating E1 and E2-deleted adenovirus encoding green fluorescent protein, at different multiplicity of infectio (MOIs). After 24 h of infection cells were trypsinised, washed, and resuspended in 300µl of PBS and analyzed for GFP expression on a fluorescence-activated cell sorter (FACS) cytometer (Dako Cytomation, Carpinteria, CA) and Summit version 4.3 software (Dako, Carpinteria, CA).
For the evaluation of Bevacizumab effects on adenoviral entry and GFP expression, KAT-4 cells were treated for 24 h with Bevacizumab and then infected for 48 h with AdGFP. Cells were harvested and prepared for FACS analysis as previously described.

3.6 Tumorigenicity assay and analysis of viral genome

All experiments were performed in six-week-old male athymic mice (Charles-River, Italy).
In the experiment performed to evaluated the effects of *dl*922-947 and *dl*1520 on ATC xenografts, 60 athymic mice were inoculated subcutaneously with 1 x 10^6 ARO or KAT-4 cells and 20 days later, when tumours were clearly detectable the animals were divided into three groups (20 animals/group) and tumour size was evaluated. Two groups received intratumorally respectively 1 x 10^8 pfu of *dl*922-947 and *dl*1520 two times per week and one group was used as control group.
To evaluate the effects of *dl*922-947 in combination with Bevacizumab KAT-4 cells ($1x10^6$) were injected into the right flank of 80 athymic mice. After 40 days, when tumours were clearly detectable, the animals were divided into four groups (20 animals/group), and tumour volume was evaluated. Two groups received Bevacizumab (5 mg/Kg/mouse) intraperitoneally (i.p.) the day 0 and 6, and the day 2 and 4 *dl*922-947 (2,5 x 10^6 pfu) was injected in the peritumoural area in a group treated with Bevacizumab and in an untreated group. This treatment was repeated for 4 week.
Tumour diameters were measured with calipers every day until the animals were killed. Tumour volumes (V) were calculated by the formula of rotational ellipsoid: V= A x B2/2 (A= axial diameter, B= rotational diameter). No mouse showed signs of wasting or other visible indications of toxicity. All mice were maintained at the Dipartimento di Biologia e Patologia Animal Facility. Animal experimentations described here have been conducted in accordance with accepted standards of animal care and in accordance with the Italian regulations for the welfare of animals used in studies of experimental neoplasia, and the study was approved by our institutional committee on animal care.
To evaluate the genome equivalent copies of *dl*922-947 and *dl*1520 in tumour xenografts, 3 animals bearing ARO or KAT-4 tumour xenografts were injected in the peritumoral area with *dl*1520 or *dl*922-947 (1 x 10^8 pfu). After 48 hours treated and control animals were sacrificed, tumours excised, viral DNA

extracted using a QIAamp DNA mini kit (Valencia, CA, USA) and viral replication evaluated by Real-time PCR using adeno hexon primers.
To evaluate the genome equivalent copies of *dl*922-947 in animals treated with Bevacizumab and *dl*922-947, KAT-4 cells ($1x10^6$) were injected into the right flank of 10 athymic mice. After 20 days, when tumours were clearly detectable animals were divided in two groups. A group received Bevacizumab (5 mg/kg/mouse) i.p. two times, at day 0 at day 5, and at day 6 *dl*922-947 ($1 x10^8$ pfu) was injected in the peritumoural area. After 48 hours animals of both groups were sacrificed, tumours excised, viral DNA extracted using a QIAamp DNA mini kit (Valencia, CA, USA) and viral replication evaluated by Real Time PCR using adeno hexon primers.

3.7 Tissue preparation and confocal microscopy

KAT-4 cells ($1x10^6$ cells) were injected into the right flank of 20 athymic mice, and after 20 days, when tumours were clearly detectable, animals were randomised into two groups (10 animals/group). Bevacizumab (5 mg/kg/mouse) was administered i.p. only in one group and after 5 days both groups received the administration of AdGFP ($1 x 10^8$ pfu) within the tumour. At the end of experiment the animals were sacrificed and the tumour were excised, snap frozen in liquid nitrogen and cut with a cryostat in thick sections for microscopic investigation. Sections were mounted onto untreated slides and coverslipped in Slow fade™ antifade (Molecular Probes) for microscopic investigation. Ten sections were sampled across the entire tumour mass to ensure they were representative of the distribution of GFP positive signal into the tumour mass. For each slice ten images at high resolution were sampled from the periphery to the core of the section.
Images were acquired using a Zeiss LSM 510 Meta argon/krypton laser scanning confocal microscope, with fluorescence excitation lines 488 nm and emission filter BP505-550, a x20 and x63 oil immersion (PlanApochromat, NA = 1.4, Zeiss) objectives, pixel depth 12 bit, , fixed box sizes of 512 x 512 pixels, pinhole below 1 Airy unit. Four images from each optical section were averaged to improve the signal to noise ratio. The colour scheme used was green for GFP-labeled structures.

3.8 Detection of cell surface coxsackie-adenovirus receptor (CAR)

The methods is described in detail in the publication at the end of the references.

3.9 Human thyroid tissue samples and Real Time RT-PCR

The methods is described in detail in the publication at the end of the references.

3.10 Protein extraction and Western blot analysis

The methods is described in detail in the publication at the end of the references.

3.11 Statistical analysis

Comparisons among different treatment groups in the experiments *in vivo* were made by the ANOVA method and the Bonferroni post hoc test using a commercial software (GraphPad Prism 4). Assessment of differences among rate of tumour growth in mice was made for each time point of the observation period. The analysis of the cell killing effect *in vitro* was also made by ANOVA method and the Bonferroni post hoc test. For all the other experiments comparisons among groups were made by ANOVA method and *t test*.

4. RESULTS AND DISCUSSION

The efficacy of oncolytic adenoviruses as therapeutic agents relies on the capability of target neoplastic cells to bind, internalize, and sustain the replication of adenoviruses. I analyzed the infectivity of a panel of human thyroid carcinoma cell lines with a GFP transducing adenovirus (AdGFP), using increasing concentration from 1 pfu to 100 pfu. The results are shown in Fig. 7

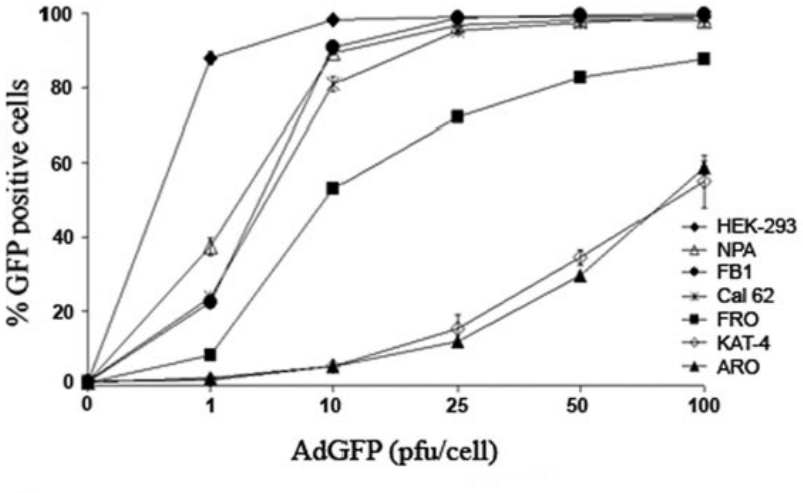

Figure 7: Adenoviral infectivity in human thyroid carcinoma cell lines
ATC cell lines ARO and KAT-4 are the less sensitive to AdGFP infection at all MOIs used, whereas FRO and Cal62 cells display a higher percentage of GFP-expressing cells. Follicular thyroid carcinoma cell line FB1 and papillary thyroid carcinoma cell line NPA show about 90% of GFP-positive cells at 10 MOI. HEK-293 cells were used as a positive control

The anaplastic thyroid carcinoma cell lines ARO, FRO, and KAT-4 display the lowest percentage of fluorescent cells at all the multiplicity of infection (MOIs) used; indeed 100 pfu/cell are required to obtain greater than 50% ARO and KAT-4 positive cells, whereas at 10 pfu/cell, about 50% of FRO cells are positive. Conversely, follicular thyroid carcinoma cell line FB1 and papillary thyroid carcinoma cell line NPA showed about 90% of GFP positive cells at 10 MOIs. As a positive control HEK-293 cells were used.

Because adenoviral infection occurs via the attachment to the CAR (Coyne et al. 2005), we analyzed CAR expression by Western blot; two CAR-specific bands of 44 and 46 kDa, respectively, were detected in all the samples (Fig. 8).

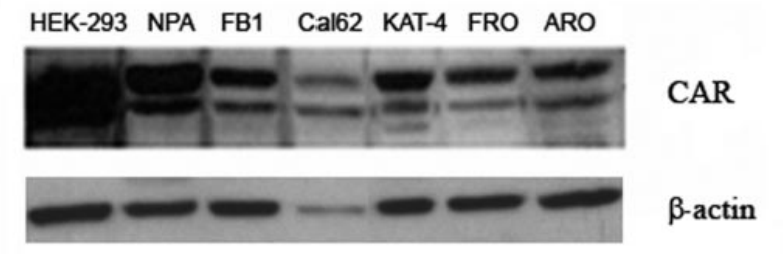

Figure 8: CAR expression in human thyroid carcinoma cell lines
Cal 62, FRO, and ARO cells show low expression of total CAR levels, whereas FB1, KAT-4, and NPA cells express the higher of total CAR levels. Equal amounts of protein lysates (50 μg) were loaded.

However, certain differences were observed in their levels; in ATC cell lines, variable levels ranging from very low to intermediate were observed; the papillary thyroid carcinoma-derived NPA cell line, the follicular carcinoma-derived FB-1 cell lines, and the ATC-derived KAT-4 cell line express the highest CAR levels.

A cytofluorimetric analysis was performed to evaluate the presence of CAR on the cell membrane (Fig. 9).

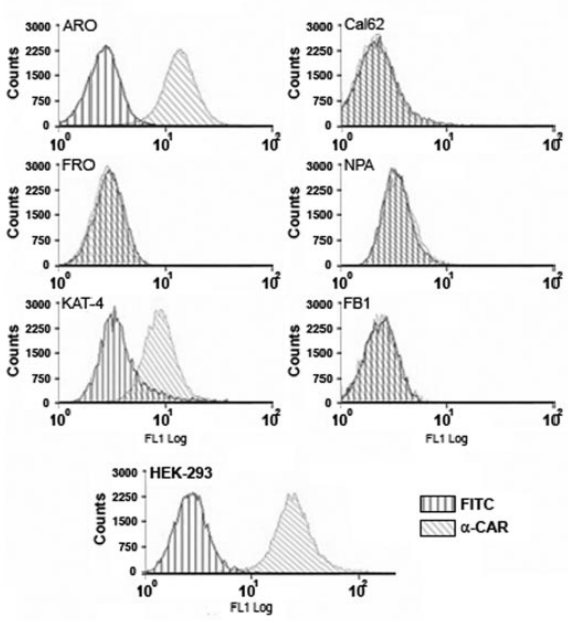

Figure 9: Cytofluorimetric analysis of CAR expression on the membrane of thyroid carcinoma cell lines
Flow cytometry analysis shows the absence of cell surface CAR expression in FRO, NPA, Cal 62, and FB1 thyroid cancer cell lines. ARO and KAT-4 cell lines show the presence of CAR on the membrane. HEK-293 cells were used as positive control.

The result shows the absence of CAR on the cell surface in FRO, NPA, Cal 62, and FB1 cells. This observation suggests a CAR-independent entry of AdGFP in these cell lines. The cell lines ARO and KAT-4 show the presence of CAR on the cell membrane despite being the less susceptible to adenoviral infection.

To confirm that anaplastic thyroid carcinomas express low levels of CAR, we evaluated the CAR mRNA levels in human thyroid carcinoma tissues by RT-PCR. Significantly lower levels (**P<0.01) in CAR gene expression were observed in papillary carcinomas, follicular carcinomas, and anaplastic thyroid carcinomas with respect to normal thyroid samples (Fig. 10).

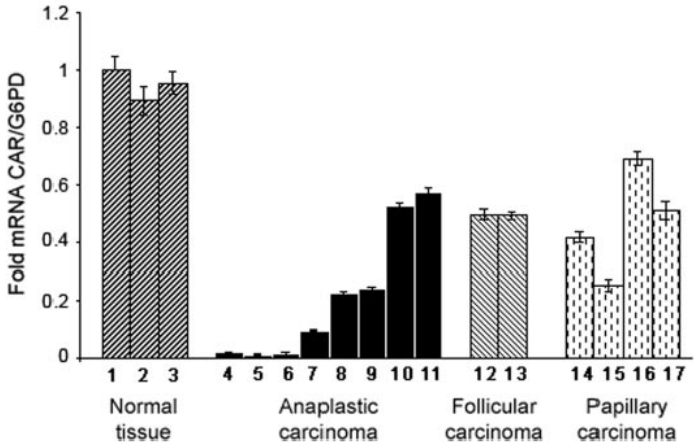

Figure 10: CAR expression in thyroid carcinoma tissues
Three normal thyroid samples (1–3), eight anaplastic (4–11), two follicular (12 and 13), and four papillary (14–17) thyroid carcinomas were used for Real-ime RT-PCR analysis of CAR expression, showing a reduction in CAR mRNA levels in all neoplastic tissues with respect to normal thyroid samples.

ATC cell lines display a low susceptibility to adenoviral infection and this was also demonstrated by our study with *dl*1520 of which high MOIs were used in all experiments (Portella et al. 2002 and 2003, Libertini et al. 2007). Therefore it is necessary to find a new oncolytic adenovirus with higher antineoplastic activity.

To this aim I have evaluated the effects of a second-generation adenoviral mutant, *dl*922-947, in the treatment of anaplastic thyroid carcinoma.
In order to show that *dl*922-947 has a higher efficiency to kill human anaplastic thyroid cell lines with respect to *dl*1520, I compared the effects of both adenoviruses on ARO, FRO, KAT-4 and also on another anaplastic carcinoma cell line, BHT-101 cells. Ad5wt virus was used as a control. Cells, seeded in 96-well plates, were infected with increasing concentrations of *dl*922-947, *dl*1520 or Ad5wt. Fig. 11 reports graphics about every cell line used in experiment. In the diagrams the percentage of cell survival is represented as a

function of used pfu/cell. In ARO, KAT-4 and BTH-101 cells *dl*922-947 has a higher cytopathic effects with respect to *dl*1520. In particular, in ARO e KAT-4 cells *dl*922-947 induces a percentage of mortality of about 90% at concentration of 0,0001 pfu/cell. In FRO cells the effects of the three adenoviruses are similar.
This first result indicates that *dl*922-947 has a higher killing efficiency against human anaplastic thyroid cell lines.

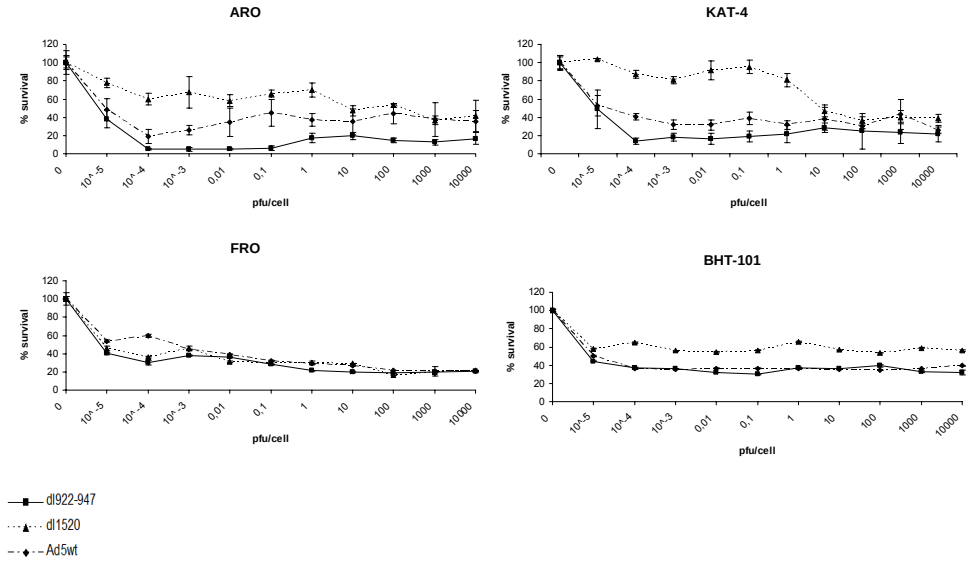

Figure 11: Cytopathic effects of *dl*922-947, *dl*1520 and Ad5wt on human anaplastic thyroid carcinoma cell lines
ARO, KAT-4, FRO and BHT-101 cells were infected with increasing concentration of *dl*922-947, *dl*1520 and Ad5wt. In ARO, KAT-4 and BTH-101 cells *dl*922-947 has a higher cytopathic effects with respect to *dl*1520 while in FRO cells the effects of the three adenoviruses are similar.

Replication of viruses into cells is a specific characteristic of their life-cycle. In order to establish if the higher degrees of cytopathic effects observed infecting ATC cells with *dl*922-947 are due to the more efficient viral replication within ATC cells, I have evaluated the efficiency of replication of *dl*922-947, *dl*1520 and Ad5wt on ARO, KAT-4, FRO and BHT-101 cells. These cells were infected respectively with a MOIs of 0,1 pfu, 1 pfu, and 100 pfu of *dl*922-947, *dl*1520 and Ad5wt. After 48 h of infection the amount of viruses genome was quantified by Real-Time PCR using specific primers for the amplification of 143 bp sequence of the viral hexon gene. Fig. 12 shows graphics relative to every cell line used in experiment. The amount of viral DNA, expressed in log scale, is reported on y-axis. The viral genome copies analysis shows higher levels of *dl*922-947 replication with respect to *dl*1520 in ARO cells, at MOIs of 1 pfu and 100 pfu (**$p<0,01$). In KAT-4 cells a

significant difference (*p<0,05), between the replication of *dl*922-947 and *dl*1520, is present only at MOI of 0,1 pfu unlike BHT-101 cells which have a significant difference (*p<0,05) at MOI of 1 pfu. In FRO cells, in which *dl*922-947 and *dl*1520 induce the same cytopathic effects, *dl*922-947 has a higher efficiency of replication with respect to *dl*1520 at MOIs of 1 pfu and 100 pfu (**p<0,01). Since in FRO cells no significant differences were observed in cell killing, it is possible that other mechanisms, besides viral replication, are involved.
These results demonstrate that *dl*922-947 has a higher replication and killing efficiency with respect to *dl*1520 in ATC cell lines, confirming its greater potentiality with respect to *dl*1520.

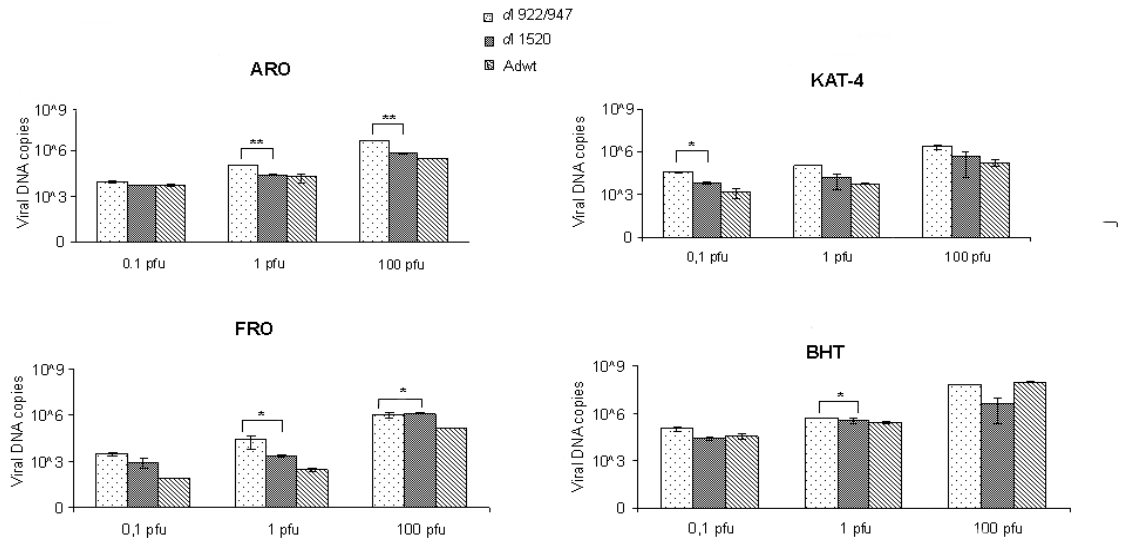

Figure 12: Adenoviruses replication on ATC cell lines
Viral DNA copies of ARO, KAT-4, FRO and BHT-101 cells infected respectively with a MOI of 0,1 pfu, 1 pfu, and 100 pfu of *dl*922-947, *dl*1520 and Ad5wt. *dl*922-947 has a higher replication efficiency with respect to *dl*1520 in all ATC cell lines (*p<0,05; **p<0,001).
It is important to note that in all cell lines the differences of the amount of viral DNA copies between *dl*922-947 and Ad5wt are significant (p<0,05; p<0,001)

In order to analyze the viral life-cycle in infected ATC cells I selected two adenoviral genes, *E1A 13 S* and *Penton,* whose expression is correlated respectively with early and late stage of the adenoviral life-cycle. I have analyzed the expression of these genes in ARO and KAT-4 cells infected respectively with MOIs of 10 pfu of *dl*1520, *dl*922-947 and Ad5wt. After 24 h of infection, the expression levels of *E1A 13 S* and *Penton* were measured by Real Time RT PCR using the forward and the reverse primers for each gene.

Expression levels of *E1A 13 S* and *Penton* are reported in Fig. 13. Genes expression levels are expressed in arbitrary units with respect to the β-actin gene used as control gene.

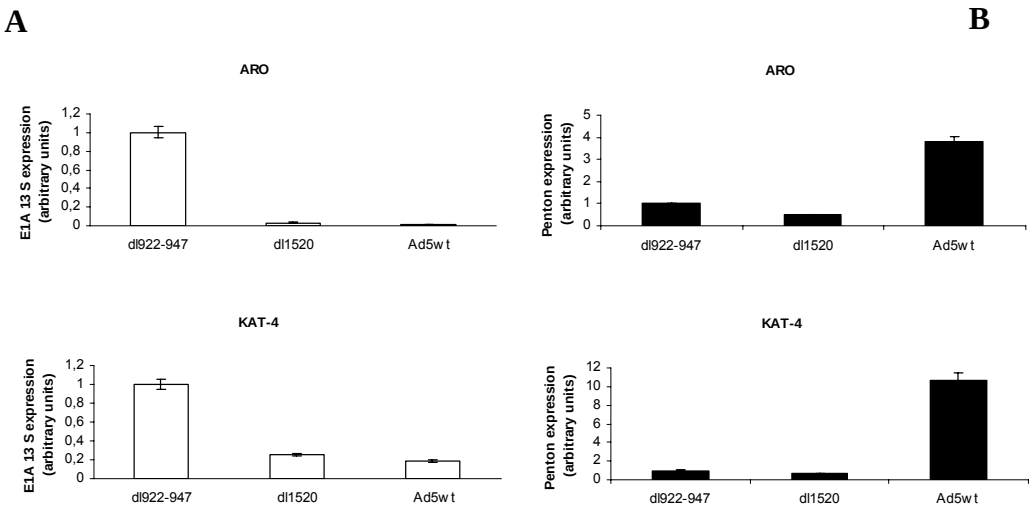

Figure 13: *E1A 13 S* and *Penton* expression levels on ARO and KAT-4 cells
A) In ARO cells the infection with *dl*922-947 induces an *E1A 13 S* expression ten fold greater with respect to *dl*1520 and Ad5wt; in KAT-4 cells expression levels of *E1A 13 S* are five fold greater after *dl*922-947 infection with respect to *dl*1520 and Ad5wt. Expression levels of *E1A 13 S* are expressed in arbitrary units respect to the β-actin gene used as control gene.
B) In ARO cells the infection with Ad5wt induces a late gene expression four fold higher with respect to *dl*922-947 and *dl*1520; in KAT-4 cells Ad5wt induces a *Penton* expression ten fold greater with respect to the other adenoviruses. Expression levels of *E1A 13 S* are expressed in arbitrary units respect to the β-actin gene used as control gene.

In ARO cells the infection with *dl*922-947 induces an *E1A 13 S* expression ten fold greater with respect to *dl*1520 and Ad5wt; in KAT-4 cells expression levels of *E1A 13 S* are five fold greater after *dl*922-947 infection with respect to *dl*1520 and Ad5wt (Fig. 13 A). In ARO cells the infection with Ad5wt induces a *Penton* gene expression four fold higher with respect to *dl*922-947 and *dl*1520; in KAT-4 cells Ad5wt induces a *Penton* expression ten fold greater with respect to the other adenoviruses (Fig. 13 B). This results show a different early and late gene expression after infection with three adenoviruses; *E1A 13 S* gene is highly expressed after *dl*922-947 infection, while *Penton* gene is more expressed after Ad5wt infection. This discrepancy could be explain considering that Ad5wt is a non-mutant adenovirus. In fact in wt adenovirus the expression of early genes is switched off at the beginning of late gene expression (Berk 1986).

To evaluate whether *dl*922-947 inhibited the growth of ARO and KAT-4 tumour xenografts 60 athymic mice were inoculated subcutaneously ARO cells or KAT-4 cells. Twenty days later, when tumours were clearly detectable,

animals were divided in three groups. Two groups received intratumourally respectively 1 x 10^8 pfu of *dl*922-947 and *dl*1520 two times per week and one group was used as control group. Tumour diameters were measured with calipers every day until the animals were killed. In Fig. 14 effects of *dl*922-947 and *dl*1520 on ARO and KAT-4 tumours xenografts are represented.

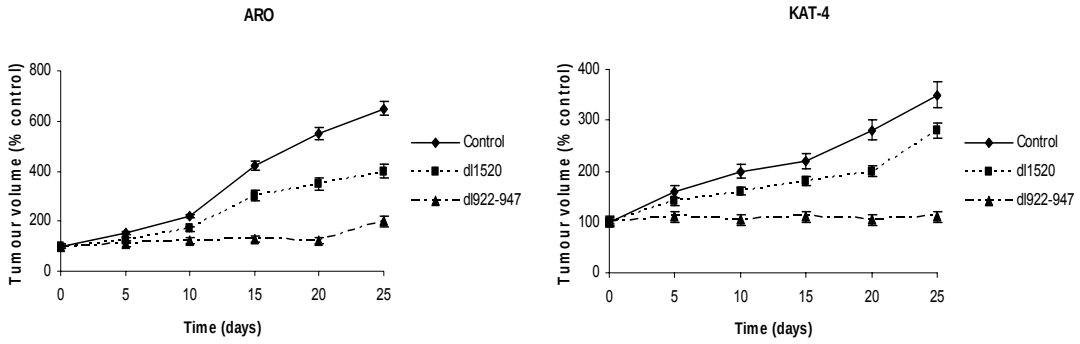

Figure 14: Inhibition of tumour growth on ARO and KAT-4 tumour xenografts
Relative tumour growth of animals treated with *dl*922-947, *dl*1520 and control groups. Starting from day 10, a significant decrease ($p<0.01$) in tumour volume was observed in *dl*922-947 treated animals with respect to the animals untreated or treated with *dl*1520

Tumour volume, expressed in percentage of control tumours volume, is reported as a function of days of treatment. Starting from day 10, a significant decrease ($p<0.01$) in tumour volume was observed in *dl*922-947 treated animals with respect to the animals untreated or treated with *dl*1520. The difference in tumour growth was maintained until the end of the experiment. Unfortunately, control animal were sacrificed being the tumours too large and the evaluation of the survival curve was not possible. None of the treated animals suffered from any clinically apparent side effects attributable to viral administration. Moreover it is important to note that in 10% of the animals treated with *dl*922-947 a complete eradication of the tumour was obtained (data non shown).

Next I have evaluate the replication of *dl*922-947 into the tumours. Three animals bearing ARO or KAT-4 tumour xenografts were injected in the peritumoural area with *dl*1520 or *dl*922-947 (1 x 10^8 pfu). After 48 hours treated and control animals were sacrificed, tumours excised, viral DNA extracted and viral replication evaluated by Real-time PCR using specific primers for the amplification of 143 bp sequence of the viral hexon gene. In Fig. 15 the amount of viral DNA copies from ARO and KAT-4 tumours, is represented.

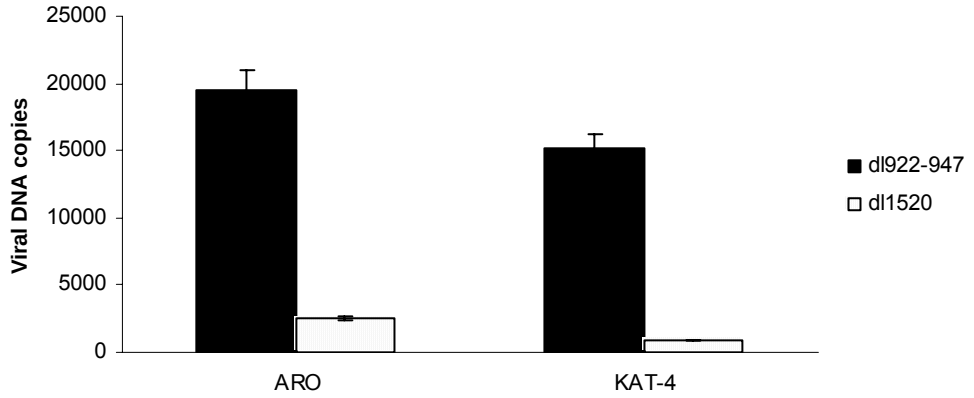

Figure 15: Adenoviruses replication in ARO and KAT-4 tumour xenografts
Genome equivalent copies of animals treated with *dl*922-947 and *dl*1520 groups. In both ARO and KAT-4 tumours *dl*922-947 has a higher efficiency of replication with respect to *dl*1520.

In both ARO and KAT-4 tumours *dl*922-947 has a higher efficiency of replication with respect to *dl*1520. This result indicates that the inhibition of tumour growth and efficiency of viral replication are events strictly correlated.
The results obtained *in vitro* and *in vivo* confirm that *dl*922-947 has a higher killing efficiency with respect to *dl*1520 and encourage to use *dl*922-947 in ATC treatment.

It is unlikely that *dl*922-947 could be used as monotherapy, therefore, to enhance its therapeutic potential, I have proposed a therapeutic strategy based on combination *dl*922-947 plus paclitaxel, a mitotic inhibitor used in cancer chemotherapy. It is well know that paclitaxel is able to induce a G2/M arrest in cell cycle, moreover it has been reported that paclitaxel potentiates adenoviral oncolysis in non-small-cell lung cancer cells (AbouEl Hassan MA et al. 2006) and it is able to cause death in anaplastic thyroid cell lines (Pushkarev VM et al. 2004). Furthermore paclitaxel enhances the effects of the oncolytic adenovirus *dl*1520 against ATC cells (Portella et al. 2003).

ARO and KAT-4 cells were exposed to increasing concentrations of paclitaxel from 0,075 ng/ml to 2 ng/ml, alone or in combination with increasing concentrations of *dl*922-947 from 0,05 pfu/cell to 2,5 pfu/cell. Fig 16 reports the percentage of cell survival as a function of paclitaxel concentration in ARO and KAT-4 cells. A significant increase in cell killing was achieved by paclitaxel/*dl*922-947 combination and the data are reported in the table below (table 2). This results indicate that the combination paclitaxel/*dl*922-947 has a higher killing efficiency with respect to the virus alone and this could represent a good tool for the treatment of ATC with respect to a monotherapy approach.

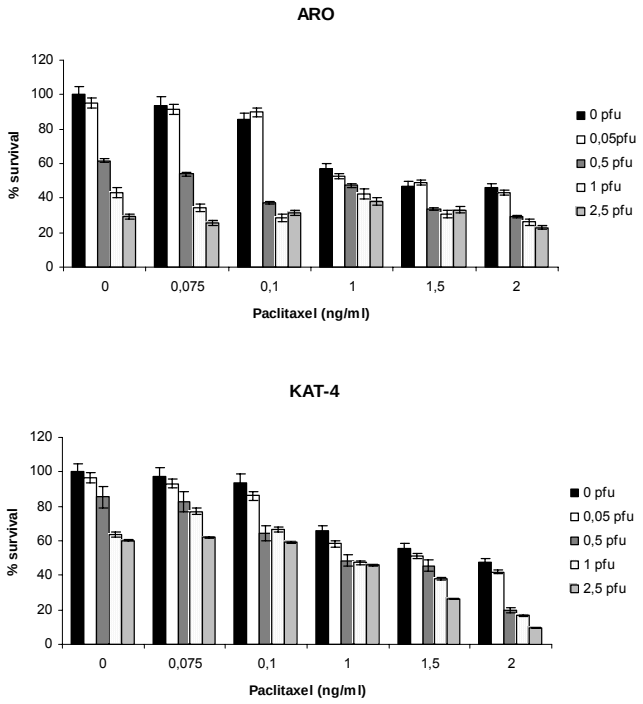

Figure 16: Effects of paclitaxel/virus combination
In ARO and KAT-4 cell the combined treatment induces a significant increase in cell killing (percentages of cell killing are reported in table 2).

Table 2: % mortality in ARO and KAT-4 cells after treatment paclitaxel plus *dl*922-947

ARO cells	**Paclitaxel 0 ng/ml**	**Paclitaxel 0,075 ng/ml**	**Paclitaxel 0,1 ng/ml**
***dl*922-947 0 pfu**	0%	6%	15%
***dl*922-947 0,5 pfu**	38%	46%	62%
***dl*922-947 1 pfu**	57%	66%	71%

KAT-4 cells	**Paclitaxel 0 ng/ml**	**Paclitaxel 0,1 ng/ml**	**Paclitaxel 1 ng/ml**	**Paclitaxel 2 ng/ml**
***dl*922-947 0 pfu**	0%	6%	34%	53%
***dl*922-947 0,05 pfu**	3%	14%	41%	//////////
***dl*922-947 0,5 pfu**	15%	35%	//////////	79%

The percentages of cell killing are expressed for the virus alone, for the paclitaxel alone and for the combination virus/paclitaxel. In blue the percentages in which is present an additive effect are indicated.

The successful application of therapeutic strategies based on replicating oncolytic viruses is limited by several obstacles and the major one is the incomplete viral dissemination within tumour mass. Compromised vascular supply and distorted functional properties of tumour vessels along with pathologically elevated tumour interstitial fluid pressure (P_{IF}) are major factors limiting drug uptake in malignant tumours (Jain 1990 and 1999, Pietras et al. 2001, Salnikov et al. 2003). Recently, a number of strategies to enhance the delivery of drugs into solid tumours have been proposed (McKee et al. 2006, Cairns et al. 2006, Minchinton and Tannock 2006). It has been suggested that vascular remodelling or normalization of tumour vessels induced by anti-angiogenic treatment could improve the delivery of viruses to tumour cells. A series of studies have been performed using anti-angiogenic therapies in ATC treatment (Prichard et al. 2007) and in particular, a study conducted on KAT-4 tumour xenografts suggests that Bevacizumab, a monoclonal antibody to VEGF, is able to reduce tumour P_{IF} (Salnikov et al. 2006).

I have proposed an approach based on combination Bevacizumab/*dl*922-947 *in vivo*. I have inoculated KAT-4 cells (1 x 10^6 cells) into the right flank of 80 athymic mice and after 40 days, when tumours were clearly detectable, animals were randomized into four groups. In two groups Bevacizumab (5 mg/kg/mouse) was administered i.p. the day 0 and 6, and the day 2 and 4 *dl*922-947 (2,5 x 10^6 pfu) was injected in the peritumoural area in a group treated with Bevacizumab and in an untreated group. This treatment was repeated for 4 week. Tumour diameters were measured with calipers every day until the animals were killed. In Fig. 17 tumour volume, expressed in percentage of volume of control tumours, is expressed as a function of days of treatment. It is important to note that since *dl*922-947 alone is able to reduce the growth of tumours in animals bearing ATC cells, a lower concentration of *dl*922-947 was used in this experiment with respect to the ones used in experiment shown in Fig. 14, in order to better evaluate the difference between the virus alone, and the virus in combination with Bevacizumab. The result shows that the combined treatment, Bevacizumab plus *dl*922-947, has a higher efficiency to reduce tumour growth with respect to the virus alone.

The pre-treatment with Bevacizumab, probably decreasing the interstitial pressure or normalizing tumour vessels, improves the delivery and the distribution of the virus into tumour mass and enhances the effect on the inhibition of tumour growth.

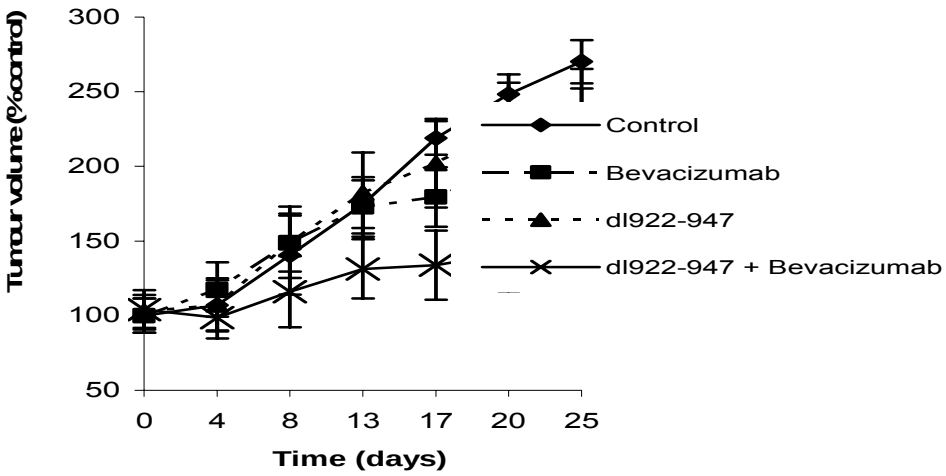

Figure 17: Effects of *dl*922-947 plus Bevacizumab in KAT-4 tumours
Relative tumour growth of animals treated *dl*922-947, Bevacizumab, *dl*922-947 plus Bevacizumab and control groups. The combined treatment, Bevacizumab plus *dl*922-947, is able to reduce tumour growth with a higher efficiency with respect to the virus alone.

In order to evaluate viral distribution in tumour tissues, KAT-4 cells were injected into the right flank of 20 athymic mice, and after 20 days, when tumours were clearly detectable, animals were randomised into two groups. Bevacizumab (5 mg/kg/mouse) was administered i.p. only in one group and after 5 days both groups received the administration of AdGFP (1 x 10^8 pfu) within the tumour. At the end of experiment the animals were sacrificed and the tumour were excised, snap frozen in liquid nitrogen and cut with a cryostat in thick sections for microscopic investigation. Fig. 18 A reports images of confocal microscopy at different magnification; on the left the distribution of AdGFP alone is represented, on the right there is the AdGFP distribution after the pre-treatment with Bevacizumab.

Fluorescence is more diffuse and intense in animal tissues treated with AdGFP plus Bevacizumab with respect to the tissues treated with the virus alone. In Fig. 18 B a quantitative measure of fluorescence, expressed in arbitrary units, in both treatments is shown. The combined treatment AdGFP/Bevacizumab induces a fluorescence intensity six fold higher with respect to the virus alone ($p<0,01$). This result suggests that the pre-treatment with Bevacizumab is probably able to normalize tumour vessels so that it is possible to obtain a better dissemination of the virus into the tumour mass with respect to the absence of treatment.

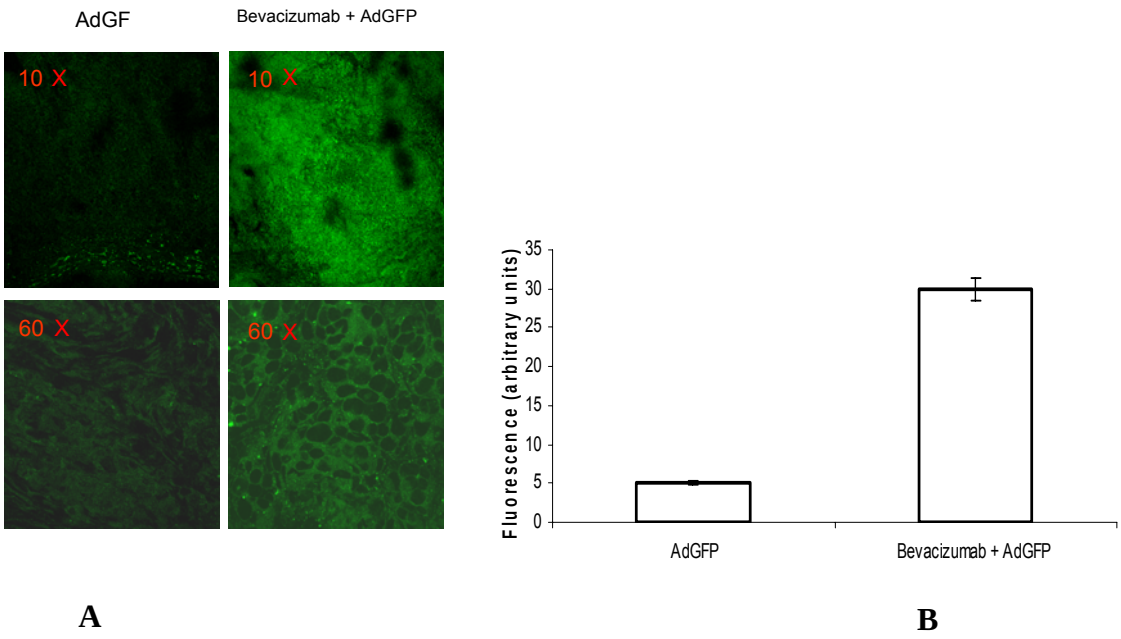

Figure 18: Effects of Bevacizumab/AdGFP combination
A) Intensity of GFP staining in tumour tissues treated with AdGFP and AdGFP plus Bevacizumab. The fluorescence is more diffuse and intense in animal tissues treated with AdGFP plus Bevacizumab with respect to the tissues treated with the virus alone. The images are at two different magnification, 10X and 60X.
B) This diagram reports a quantitative measure of fluorescence, expressed in arbitrary units. The combined treatment AdGFP/Bevacizumab induces a fluorescence intensity six fold higher with respect to the virus alone.

Next I have decide to evaluate the genome equivalent copies of *dl*922-947 in animals treated with Bevacizumab and *dl*922-947. KAT-4 cells were injected into the right flank of 10 athymic mice. After 20 days, when tumours were clearly detectable animals were divided in two groups. A group received Bevacizumab (5 mg/kg/mouse) i.p. two times, at day 0 at day 5, and at day 6 *dl*922-947 (1 x10^8 pfu) was injected in the peritumoural area. After 48 hours animals of both groups were sacrificed, tumours excised, viral DNA extracted and viral replication evaluated by Real Time PCR using the forward and the reverse primers for viral hexon gene. Fig. 19 reports the amount of viral DNA copies in the group treated with *dl*922-947 alone and in the group treated with *dl*922-947 plus Bevacizumab. The combined treatment *dl*922-947/Bevacizumab induces a viral replication six fold higher ($p<0,01$) with respect to the virus alone. All these results demonstrated that the pre-treatment with Bevacizumab is able to improve the therapeutic effect of *dl*922-947 adenovirus against ATC.

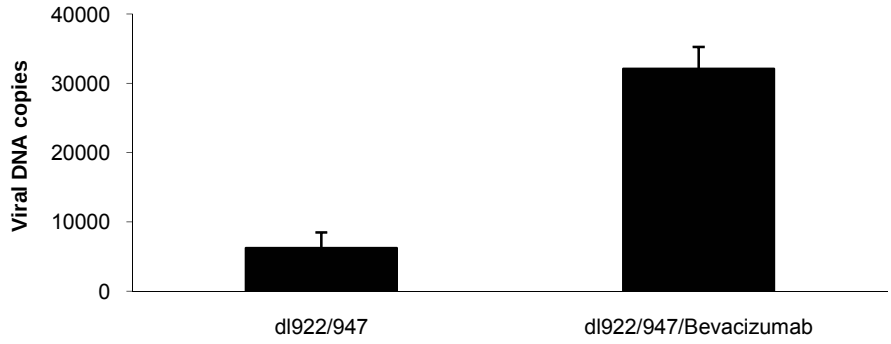

Figure 19: Effects of Bevacizumab/virus combination
Genome equivalent copies of animals treated with *dl*922-947 and *dl*922-947 plus Bevacizumab. The combined treatment *dl*922-947/Bevacizumab induces a viral replication six fold higher with respect to the virus alone.

In order to evaluate if Bevacizumab is able to produce *in vitro* the same effects observed *in vivo*, I have performed a series of experiments on KAT-4 cells.

In the first experiment I have evaluated the survival of KAT-4 cells treated for 48 h with Bevacizumab at concentrations of 0,1 μM and 0,25 μM and then infected with *dl*922-947 at MOIs of 0,01 pfu, 0,1 pfu and 1 pfu and. Fig. 20 reports the percentage of cell survival as a function of used pfu/cell. No significant differences between the combined treatment Bevacizumab/*dl*922-947 and the virus alone were observed.

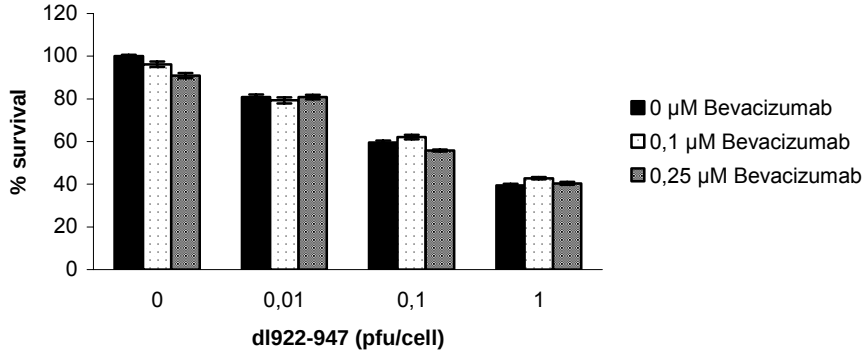

Figure 20: Combined treatment *dl*922-947 plus Bevacizumab does not increase the mortality of KAT-4 cells *in vitro*
KAT-4 cells were treated for 48 h with Bevacizumab at concentrations of 0,1 μM and 0,25 μM and then infected with *dl*922-947 at MOIs of 0,01 pfu, 0,1 pfu and 1 pfu and. No differences in the combined treatment with respect to the virus alone are observed.

Then, I have evaluated the replication efficiency of combined treatment Bevacizumab/*dl*922-947 with respect to virus alone. I treated KAT-4 cells with Bevacizumab at concentrations of 0,25 μM, 0,5 μM and 1 μM and after 48 h I infected cells with *dl*922-947 at MOIs of 1 pfu and 10 pfu. After infection the amount of viruses genome was quantified by Real-Time PCR using specific primers for the viral hexon gene. Fig. 21 reports the amount of viral DNA copies as a function of used pfu/cell. No significant differences between the replication of the virus alone and the virus in combination with Bevacizumab were observed.

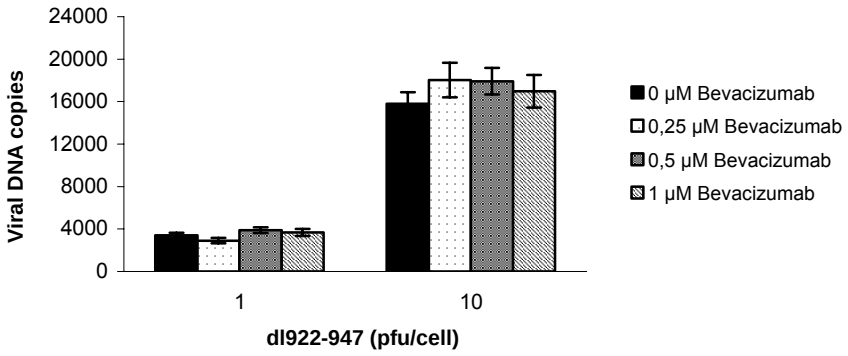

Figure 21: Combined treatment *dl*922-947/Bevacizumab does not increase viral replication in KAT-4 cells *in vitro*
KAT-4 cells were treated with Bevacizumab at concentrations of 0,25 μM, 0,5 μM and 1 μM and after 48 h were infected with *dl*922-947 at MOIs of 1 pfu and 10 pfu. After infection the amount of viruses genome was quantified by Real-Time PCR. No differences in the combined treatment with respect to the virus alone are observed.

Finally, I have performed a FACS analysis in order to evaluate the infectivity of KAT-4 cells in presence of Bevacizumab. KAT-4 cells were pre-treated with two concentrations of Bevacizumab (0,5 μM and 1 μM) for 48 h and then infected with AdGFP at MOIs of 100 pfu, 200 pfu and 300 pfu. Fig. 22 reports the fluorescence emission, expressed in arbitrary units, as a function of used pfu/cell. FACS analysis showed that Bevacizumab treatment does not induce an increase in the infectivity of KAT-4 cells.
The data obtained treating *in vitro* KAT-4 cells with Bevacizumab and *dl*922-947, demonstrate that the effects of inhibition of tumour xenografts growth are not due to a direct activity on ATC cells. It is possible that the effects observed treating ATC xenografts with Bevacizumab and *dl*922-947 are due to an activity against tumour stroma cells.

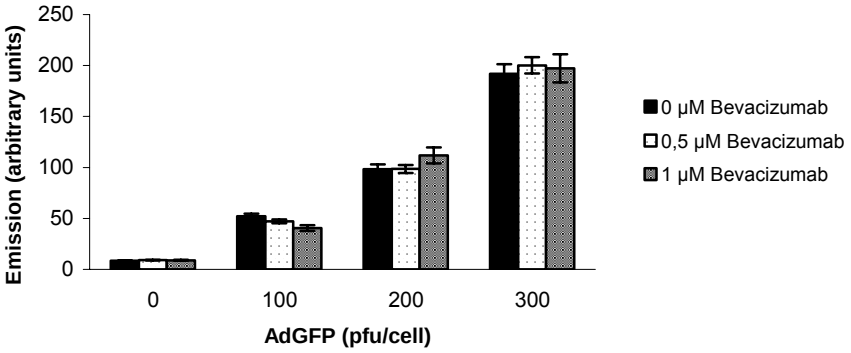

Figure 22: Combined treatment AdGFP/Bevacizumab does not increase the infectivity in KAT-4 cells

KAT-4 cells were pre-treated with two concentrations of Bevacizumab (0,5 µM and 1 µM) for 48 h and then infected with AdGFP at MOIs of 100 pfu, 200 pfu and 300 pfu. No differences, in the infectivity of KAT-4 cells, in the combined treatment with respect to the virus alone are observed.

5. CONCLUSIONS

Anaplastic thyroid carcinoma (ATC) is one of the most lethal human neoplasia and the absence of active therapies is the major impediment to the successful control of the disease.

In this study I have proposed a novel therapeutic approaches based on the use of oncolytic adenoviruses and in particular of a second-generation adenoviral mutant, *dl*922-947. I showed that *dl*922-947 had a greater cytopathic effect with respect to *dl*1520, an oncolytic virus already in clinical trials and *dl*922-947 showed also a superior efficiency with respect to *dl*1520 against ATC tumour xenografts. These data suggest that *dl*922-947 could represent a better option for virotherapy of ATC with respect to *dl*1520.

It is well known that the successful application of therapeutic strategies based on replicating oncolytic viruses is limited by several obstacles and the major one is the incomplete viral dissemination within tumour mass. Since it has been suggested that vascular remodelling or normalization of tumour vessels induced by anti-angiogenic treatment could improve the delivery of viruses to tumour cells, in this study I have proposed a therapeutic strategy based on the use of Bevacizumab, a recombinant humanized monoclonal antibody to the VEGF, in combination with *dl*922-947. The results of experiments showed that the combined treatment Bevacizumab plus *dl*922-947 enhanced the antineoplastic effects of the virus against ATC xenografts. Moreover, the analysis of viral distribution performed treating animals bearing KAT-4 tumour xenografts with Bevacizumab and then injecting the AdGFP within the tumour, confirmed that Bevacizumab pre-treatment improved the distribution within the tumour since a more intense GFP staining was observed in all tumour tissues. Finally the data obtained treating *in vitro* KAT-4 cells with Bevacizumab and *dl*922-947, indicated that the effects of inhibition of tumour xenografts growth were not due to a direct activity on ATC cells but to a direct activity on tumour stroma.

In conclusion, the results described in this study encourage the use of the *dl*922-947 virus for new therapeutic protocols for the treatment of ATC and in particular a combination between the virus and anti-angiogenic treatment could represent a better option for virotherapy against this very aggressive carcinoma.

6. ACKNOWLEDGEMENTS

I thank Prof Giancarlo Vecchio, my coordinator, who gave me the possibility to take part in this PhD program.

I thank Prof Giuseppe Portella, my tutor, who gave me the opportunity to work on a very interesting project and for his constant support.

I thank Dr Silvana Libertini, not only a colleague but a friend who helped me in every moment of this period.

I thank all the people of the laboratory who gave me friendship and suggestions.

I'm really grateful to my parents Aldo and Laura, my sisters Sara and Paola, my boyfriend Giancarmine and all my friends, who give me love and encouragement in every moment of my life.

7. REFERENCES

- AbouEl Hassan MA, Braam SR, Kruyt FA. Paclitaxel and vincristine potentiate adenoviral oncolysis that is associated with cell cycle and apoptosis modulation, whereas they differentially affect the viral life cycle in non-small-cell lung cancer cells. Cancer Gene Ther. 2006; 13(12): 1105-14.
- Aoyagi M, Higashino F, Yasuda M, Takahashi A, Sawada Y, Totsuka Y, Kohgo T, Sano H, Kobayashi M, Shindoh M. Nuclear export of adenovirus E4orf6 protein is necessary for its ability to antagonize apoptotic activity of BH3-only proteins. Oncogene 2003; 22:6919–27
- Asada T. Treatment of human cancer with mumps virus. Cancer 1974; 34:1907–1928.
- Baish JW, Jain RK. Fractals and cancer. Cancer Res. 2000; 60:3683–3688
- Bergelson JM, Cunningham JA, Droguett G, Kurt-Jones EA, Krithivas A, Hong JS, Horwitz MS, Crowell RL, Finberg RW. Isolation of a common receptor for Coxsackie B viruses and adenoviruses 2 and 5. Science (Wash DC) 1997; 275:1320–3.
- Berk AJ Adenovirus promoters and E1A transactivation. Annu. Rev. Genet. 1986; 20: 45–79.
- Bischoff JR, Kirn DH, Williams A, Heise C, Horn S, Muna M, Ng L, Nye JA, Sampson-Johannes A, Fattaey A, McCormick F. An adenovirus mutant that replicates selectively in p53-deficient human tumor cells. Science (Wash DC) 1996; 274:373–6.
- Cairns R, Papandreou I, Denko N. Overcoming physiologic barriers to cancer treatment by molecularly targeting the tumor microenvironment, Mol. Cancer Res. 2006; 4:61–70.
- Cassel WA, Garrett RE. Newcastle disease virus as an antineoplastic agent. Cancer 1965; 18:863–868.
- Chakravarti D, Ogryzko V, Kao HY, Nash A, Chen H, Nakatani Y, Evans RM. A viral mechanism for inhibition of p300 and PCAF acetyltransferase activity. Cell 1999; 96:393 – 403.
- Chen Y, DeWeese T, Dilley J, et al. CV706, a prostate cancerspecific adenovirus variant, in combination with radiotherapy produces synergistic antitumor efficacy without increasing toxicity. Cancer Res 2001; 61:5453–60
- Chiocca AE. Oncolytic viruses. Nat Rev Cancer 2002; 2:938−950
- Coffey MC, Strong JE, Forsyth PA, Lee PW. Reovirus therapy of tumors with activated Ras pathway. Science 1998; 282:1332- 1334.
- Coyne CB, Bergelson JM. CAR: a virus receptor within the tight junction. Adv Drug Deliv Rev 2005; 57: 869–882

- Crompton AM, Kirn DH. From ONYX-015 to armed vaccinia viruses: the education and evolution of oncolytic virus development. Curr Cancer Drug Targets. 2007; 2:133-139
- De Jong RN, Van Der Vliet PC, Brenkman AB. Adenovirus DNA replication: Protein priming, jumping back and the role of the DNA binding protein DBP. Curr. Top. Microbiol. Immunol. 2003; 272:187–211.
- Debbas M, White E. Wild-type p53 mediates apoptosis by E1A, which is inhibited by E1B. Genes Dev. 1993; 7:546–554.
- Dmitriev I, Kashentseva E, Rogers BE, Krasnykh V, Curiel DT. Ectodomain of coxsackievirus and adenovirus receptor genetically fused to epidermal growth factor mediates adenovirus targeting to epidermal growth factor receptor-positive cells. J Virol. 2000; 74(15): 6875-84
- Duncan MR, Stanish SM, Cox DC. Differential sensitivity of normal and transformed human cells to reovirus infection. J Virol 1978 ;28:444-449.
- El-Deiry WS, Tokino T, Velculescu VE,. Levy DB, Parsons R, Trent JM, Lin K, Mercer WE, Kinzler KW, Vogelstein B. WAF-1, a potential mediator of p53 tumor suppression. Cell 1993; 75:817–825.
- Ferrara N, Hillan KJ, Gerber HP, Novotny W. Discovery and development of bevacizumab, an ant-VEGF antibody for treating cancer. Nat Rev Drug Discov 2004; 3:391–399.
- Fields BN, Knipe DM, Howley PM. Fields virology. Philadelphia: Lippincott-Raven, 1996.
- Fueyo J, Gomez-Manzano C, Alemany R, et al. A mutant oncolytic adenovirus targeting the Rb pathway produces anti-glioma effect in vivo. Oncogene 2000; 19:2–12.
- Fueyo J, Gomez-Manzano C, Alemany R, Lee PS, McDonnell TJ, Mitlianga P, Shi YX, Levin VA, Yung WK, Kyritsis AP. A mutant oncolytic adenovirus targeting the Rb pathway produces anti-glioma effect in vivo. Oncogene 2000; 19:2–12.
- Gallimore PH, Turnell AS. Adenovirus E1A: remodelling the host cell, a life or death experience. Oncogene 2001; 20:7824–35
- Geoerger B, Grill J, Opolon P, Morizet J, Aubert G, Lecluse Y, van Beusechem VW, Gerritsen WR, Kirn DH, Vassal G. Potentiation of radiation therapy by the oncolytic adenovirus dl1520 (ONYX-015) in human malignant glioma xenografts. Br J Cancer 2003; 89:577–84.
- Geoerger B, Grill J, Opolon P, Morizet J, Aubert G, Terrier-Lacombe MJ, Bressac De-Paillerets B, Barrois M, Feunteun J, Kirn DH, Vassal G. Oncolytic activity of the E1B-55 kDa-deleted adenovirus ONYX-015 is independent of cellular p53 status in human malignant glioma xenografts. Cancer Res 2002; 62:764–72.

- Gerber HP, Ferrara N. Pharmacology and pharmacodynamics of bevacizumab as monotherapy or in combination with cytotoxic therapy in preclinical studies. Cancer Res 2005; 65:671–680
- Goodrum FD, Ornelles DA. p53 status does not determine outcome of E1B 55-kilodalton mutant adenovirus lytic infection. J Virol 1998; 72:9479–90
- Gordon MS, Margolin K, Talpaz M, Sledge GW Jr, Holmgren E, Benjamin R, Stalter S, Shak S, Adelman D. Phase I safety and pharmacokinetic study of recombinant human anti-vascular endothelial growth factor in patients with advanced cancer. J Clin Oncol 2001; 19:843–850.
- Haigh PI, Ituarte PH, Wu HS, Treseler PA, Posner MD, Quivey JM, Duh QY, Clark OH. Completely resected anaplastic thyroid carcinoma combined with adjuvant chemotherapy and irradiation is associated with prolonged survival. Cancer 2001; 91:2335–42.
- Hall AR, Dix BR, O'Carroll SJ, Braithwaite AW. p53-dependent cell death/apoptosis is required for a productive adenovirus infection. Nat Med 1998; 4:1068–72.
- Hallenbeck PL, Chang YN, Hay C, Golightly D, Stewart D, Lin J, Phipps S, Chiang YL. A novel tumor-specific replication-restricted adenoviral vector for gene therapy of hepatocellular carcinoma. Hum Gene Ther 1999; 10:1721–33.
- Hamamori Y, Sartorelli V, Ogryzko V, Puri PL, Wu HY, Wang JY, Nakatani Y, Kedes L. Regulation of histone acetyltransferases p300 and PCAF by the BHLH protein Twist and adenoviral oncoprotein E1a. Cell 1999; 96:405 – 413.
- Harada JN, Berk AJ. p53-Independent and -dependent requirements for E1B–55K in adenovirus type 5 replication. J Virol 1999; 73:5333–44.
- Harlow E, Whyte P, Franza BR jr, Schley C. Association of adenovirus early-region 1A proteins with cellular polypeptides. Mol. Cell. Biol 1986; 6:1579–1589.
- Hashiro G, Loh PC, Yau JT. The preferential cytotoxicity of reovirus for certain transformed cell lines. Arch Virol 1977; 54:307-315.
- Heise C, Hermiston T, Johnson L, Brooks G, Sampson-Johannes A, Williams A, Hawkins L, Kirn D. An adenovirus E1A mutant that demonstrates potent and selective systemic anti-tumoral efficacy. Nat Med 2000; 6:1134–9.
- Hirasawa K, Nishikawa SG, Norman KL, Coffey MC, Thompson BG, Yoon CS, Waisman DM, Lee PW. Systemic reovirus therapy of metastatic cancer in immune-competent mice. Cancer Res. 2003; 63(2):348-53.
- Hsieh CL, Yang L, Miao L, Yeung F, Kao C, Yang H, Zhau HE, Chung LW. A novel targeting modality to enhance adenoviral replication by

vitamin D(3) in androgen-independent human prostate cancer cells and tumors. Cancer Res 2002; 62:3084–92.

- Hundahl SA, Fleming ID, Fremgen AM, Menck HR. A national cancer data base report on 53 856 cases of thyroid carcinoma treated in the US, 1985–1995. Cancer 1998; 83:2638–48.
- Hurwitz H, Fehrenbacher L, Novotny W, Cartwright T, Hainsworth J, Heim W, Berlin J, Baron A, Griffing S, Holmgren E, Ferrara N, Fyfe G, Rogers B, Ross R, Kabbinavar F. Bevacizumab plus irinotecan, fluorouracil, and leucovorin for metastatic colorectal cancer. N Engl J Med 2004; 350:2335–2342.
- Jain RK. Physiological barriers to delivery of monoclonal antibodies and other macromolecules in tumours. Cancer Res 1990; 50:814s–819s.
- Jain RK. Transport of molecules, particles, and cells in solid tumours. Annu Rev Biomed Eng 1999; 1:241–63.
- Kao CC, Yew PR, Berk AJ. Domains required for in vitro association between the cellular p53 and the adenovirus 2 E1B 55kD proteins. Virology 1990; 179:806–814.
- Kirn D. Clinical research results with *dl*1520 (Onyx-015), a replication-selective adenovirus for the treatment of cancer: What have we learned? Gene Ther. 2001; 8:89–98.
- Kruyt FA, Curiel DT. Toward a new generation of conditionally replicating adenoviruses: pairing tumor selectivity with maximal oncolysis. Hum Gene Ther 2002; 13:485-95.
- Lamfers ML, Grill J, Dirven CM, et al. Potential of the conditionally replicative adenovirus Ad5-Delta24RGD in the treatment of malignant gliomas and its enhanced effect with radiotherapy. Cancer Res. 2002; 62:5736–42.
- Libertini S, Iacuzzo I, Ferraro A, Vitale M, Bifulco M, Fusco A, Portella G. Lovastatin enhances the replication of the oncolytic adenovirus *dl*1520 and its antineoplastic activity against anaplastic thyroid carcinoma cells. Endocrinology 2007;148(11): 5186-94.
- Lockley M, Fernandez M, Wang Y, Li NF, Conroy S, Lemoine N, McNeish I. Activity of the Adenoviral E1A Deletion Mutant dl922-947 in Ovarian Cancer: Comparison with E1A Wild-type Viruses, Bioluminescence Monitoring, and Intraperitoneal Delivery in Icodextrin Cancer Res 2006; 66: 989-998
- Lorence RM, Reichard KW, Katubig BB, Reyes HM, Phuangsab A, Mitchell BR, Cascino CJ, Walter RJ, Peeples ME. Complete regression of human neuroblastoma xenografts in athymic mice after local Newcastle disease virus therapy. J Natl Cancer Inst 1994; 86:1228-1233.
- Martuza RL, Malick A, Markert JM, Ruffner KL, Coen DM. Experimental therapy of human glioma by means of a genetically engineered virus mutant. Science 1991; 252:854–856

- Mastrangelo MJ, Maguire Jr HC, Eisenlohr LC, et al. Intratumoral recombinant GM-CSF-encoding virus as gene therapy in patients with cutaneous melanoma. Cancer Gene Ther. 1999; 6:409–422.
- Matsubara S, Wada Y, Gardner TA, Egawa M, Park MS, Hsieh CL, Zhau HE, Kao C, Kamidono S, Gillenwater JY, Chung LW. A conditional replication competent adenoviral vector, Ad-OC-E1a, to cotarget prostate cancer and bone stroma in an experimental model of androgen-independent prostate cancer bone metastasis. Cancer Res 2001; 61:6012–9.
- McIver B, Hay ID, Giuffrida DF, Dvorak CE, Grant CS, Thompson GB, van Heerden JA, Goellner JR. Anaplastic thyroid carcinoma: a 50-year experience at a single institution. Surgery 2001; 130:1028–34.
- McKee TD, Grandi P, Mok W, Alexandrakis G, Insin N, Zimmer JP, Bawendi MG, Boucher Y, Breakefield XO, Jain RK. Degradation of fibrillar collagen in a human melanoma xenograft improves the efficacy of an oncolytic herpes simplex virus vector. Cancer Res. 2006; 66:2509–2513.
- Minchinton AI, Tannock IF. Drug penetration in solid tumours. Nat. Rev. Cancer 2006; 6:583–592
- Mineta T, Rabkin SD, Yazaki T et al. Attenuated multimutated herpes simplex virus-1 for the treatment of malignant gliomas. Nat Med 1995;1:938 943.
- Miyashita T, Reed JC. Tumor suppressor p53 is a direct transcriptional activator of the human bax gene. Cell 1995; 80:293–299
- Moran E. DNA tumor virus transforming proteins and the cell cycle. Curr. Opin. Genet. Dev. 1993; 3:63–70.
- Nemunaitis J, Ganly I, Khuri F, Arseneau J, Kuhn J, McCarty T, Landers S, Maples P, Romel L, Randlev B, Reid T, Kaye S, Kirn D. Selective replication and oncolysis in p53 mutant tumors with ONYX-015, an E1B-55kD gene-deleted adenovirus, in patients with advanced head and neck cancer: A phase II trial. Cancer Res. 2000; 60:6359–6366.
- Nemunaitis J, Khuri F, Ganly I, Arseneau J, Posner M, Vokes E, Kuhn J, McCarty T, Landers S, Blackburn A, Romel L, Randlev B, Kaye S, Kirn, D. Phase II trial of intratumoral administration of ONYX-015, a replication-selective adenovirus, in patients with refractory head and neck cancer. J. Clin. Oncol. 2001b; 19:289–298.
- Nevins JR. Adenovirus E1A: Transcription regulation and alteration of cell growth control. Curr. Top. Microbiol. Immunol. 1995; 199: 25–32.
- O'Shea CC, Soria C, Bagus B, McCormick F. Heatshock phenocopies E1B-55K late functions and selectively sensitizes refractory tumor cells to ONYX-015 oncolytic viral therapy. Cancer Cell 2005; 8:61-74
- Okuno Y, Asada T, Yamanishi K, Otsuka T, Takahashi M, Tanioka T, Aoyama H, Fukui O, Matsumoto K, Uemura F, Wada A. Studies on

the use of mumps virus for treatment of human cancer. Biken J 1978; 21:37–49.
- Pack GT. Note on the experimental use of rabies vaccine for melanomatosis. AMA Arch. Derm. Syphilol. 1950; 62:694–695.
- Parreno M, Garriga J, Limon A, Albrecht JH, Grana X. E1A modulates phosphorylation of p130 and p107 by differentially regulating the activity of G1/S cyclin/CDK complexes. Oncogene 2001; 20:4793–4806.
- Passler C, Scheuba C, Prager G, Kaserer K, Flores JA, Vierhapper H, Niederle B. Anaplastic (undifferentiated) thyroid carcinoma (ATC). A retrospective analysis. Langenbecks Arch Surg 1999; 384:284–93.
- Pecora AL, Rizvi N, Choen GI, Meropol NJ, Sterman D, Marshall JL, Goldberg S, Gross P, O'Neil JD, Groene WS, Roberts MS, Rabin H, Bamat MK, Lorence RM. Phase I trial of intravenous administration of PV701, an oncolytic virus, in patients with advanced solid cancers. J. Clin. Oncol. 2002; 20:2251–2266.
- Petit T, Davidson KK, Cerna C, Lawrence RA, Von Hoff DD, Heise C, Kirn D, Izbicka E. Efficient induction of apoptosis by ONYX-015 adenovirus in human colon cancer cell lines regardless of p53 status. Anticancer Drugs 2002; 13:47–50.
- Pierie JP, Muzikansky A, Gaz RD, Faquin WC, Ott MJ. The effect of surgery and radiotherapy on outcome of anaplastic thyroid carcinoma. Ann Surg Oncol 2002; 9:57–64.
- Pietras K, Östman A, Sjöquist M, Buchdunger E, Reed RK, Heldin CH, Rubin K. Inhibition of platelet-derived growth factor receptors reduces interstitial hypertension and increases transcapillary transport in tumours. Cancer Res 2001; 61:2929–34.
- Pilder S, Moore M, Logan J, Shenk T. The adenovirus E1B-55K transforming polypeptide modulates transport or cytoplasmic stabilization of viral and host cell mRNAs. Mol. Cell. Biol. 1986; 6, 470–476.
- Portella G, Pacelli R, Libertini S, Cella L, Vecchio G, Salvatore M, Fusco A. ONYX-015 enhances radiation-induced death of human anaplastic thyroid carcinoma cells. J. Clin. Endocrinol. Metab. 2003; 88:5027-5032.
- Portella G, Scala S, Vitagliano D, Vecchio G, Fusco A. Onyx-015, an E1B gene-defective adenovirus, induces cell death in human anaplastic thyroid carcinoma cell lines. J Clin Endocrinol Metab. 2002; 87(6): 2525–2531
- Post DE, Khuri FR, Simons JW, Van Meir EG. Replicative Oncolytic Adenoviruses in Multimodal Cancer Regimens. Human Gene Therapy 2003; 14:933–946
- Pushkarev VM, Starenki DV, Saenko VA, Namba H, Kurebayashi J, Tronko MD, Yamashita S. Molecular mechanisms of the effects of low

concentrations of taxol in anaplastic thyroid cancer cells. Endocrinology 2004; 145(7): 3143-52.

- Qian J, Yang J, Dragovic AF, Abu-Isa E, Lawrence TS, Zhang M. Cancer Res. 2005; 65:5493-7.
- Rao L, Debbas M, Sabbatini P, Hockenbery D, Korsmeyer S, White E. The adenovirus E1A proteins induce apoptosis, which is inhibited by the E1B 19-kDa and Bcl-2 proteins. Proc. Natl. Acad. Sci. U.S.A. 1992; 89:7742–7746.
- Reichard KW, Lorence RM, Cascino CJ, Peeples ME, Walter RJ, Fernando MB, Reyes HM, Greager JA Newcastle disease virus selectively kills human tumor cells. J Surg Res 1992; 52:448-453.
- Ries SJ, Brandts CH, Chung AS, Biederer CH, Hann BC, Lipner EM, McCormick F, Korn WM. Loss of p14ARF in tumor cells facilitates replication of the adenovirus mutant *dl*1520 (ONYX-015). Nat Med 2000; 6:1128–33.
- Roberts MS, Buasen PT, Incao BA et al. PV701, a naturally attenuated strain of Newcastle disease virus, has a broad spectrum of oncolytic activity against human tumor xenografts. Proc Am Assoc Cancer Res 2001; 42:2441a.
- Rodriguez R, Schuur ER, Lim HY, Henderson GA, Simons JW, Henderson DR. Prostate attenuated replication competent adenovirus (ARCA) CN706: a selective cytotoxic for prostate-specific antigenpositive prostate cancer cells. Cancer Res 1997; 57:2559–63.
- Rothmann T, Hengstermann A, Whitaker NJ, Scheffner M, zur Hausen H. Replication of ONYX-015, a potential anticancer adenovirus, is independent of p53 status in tumor cells J Virol 1998; 72:9470–8.
- Roussel MF. The INK 4 family of cell cycle inhibitor in cancer. Oncogene 1999; 18:5311-7.
- Salnikov AV, Heldin NE,. Stuhr LB, Wiig H, Gerber H,. Reed RK, Rubin K. Inhibition of carcinoma cell-derived VEGF reduces inflammatory characteristics in xenograft carcinoma. Int. J. Cancer. 2006; 119:2795–2802
- Salnikov AV, Iversen VV, Koisti M, Sundberg C, Johansson L, Stuhr LB, Sjöquist M, Ahlström H, Reed RK, Rubin K. Lowering of tumour interstitial fluid pressure specifically augments efficacy of chemotherapy. FASEB J 2003; 17:1756–8.
- Shah AC, Benos D, Gillespie GY, Markert JM. Oncolytic viruses: clinical applications as vectors for the treatment of malignant gliomas. J. Neurooncol. 2003; 65:203–226
- Shenk T. Adenoviridae: The viruses and their replication. In Virology 1996. B.N. Fields, D.M. Knipe, and P.M. Howley, eds. (Lippincott-Raven, New York) pp. 2111–2148.

- Sherman SI. Anaplastic carcinoma: clinical aspects. In: Wartofsky L, ed. Thyroid cancer. a comprehensive guide to clinical management. Totowa, NJ: Humana Press, 1999: 319–25
- Sherr CJ. The Pezcoller lecture: cancer cell cycle revisited. Cancer Res 2000; 60:3689-95.
- Sinkovics J, Horvath J. New developments in the virus therapy of cancer: a historical review. Intervirology 1993; 36:193–214.
- Sinkovics JG, Horvath JC. Newcastle disease virus (NDV): brief history of its oncolytic strains. J. Clin. Virol. 2000; 16:1–15.
- Southam CM, Hilleman MR, Werner JH. Pathogenicity and oncolytic capacity of RI virus strain RI-67 in man. J. Lab. Clin. Med. 1956; 47:573–582.
- Southam CM, Moore AE. Clinical studies of viruses as antineoplastic agents with particular reference to Egypt 101 virus. Cancer 1952; 5:1025–1034.
- Taylor MW, Cordell B, Souhrada M, S. Prather, Viruses as an aid to cancer therapy: regression of solid and ascites tumors in rodents after treatment with bovine enterovirus, Proc. Natl. Acad. Sci. USA 68 (1971) 836–840.
- Tomko RP, Xu R, Philipson L. HCAR and MCAR: the human and mouse cellular receptors for subgroup C adenoviruses and group B coxsackieviruses. Proc Natl Acad Sci USA 1997; 94:3352–6.
- Wakimoto H, Fulci G, Tyminski E, Chiocca EA. Altered expression of antiviral cytokine mRNAs associated with cyclophosphamide's enhancement of viral oncolysis. Gene Ther. 2004; 11:214–23
- Xia ZJ, Chang JH, Zhang L, Jiang WQ, Guan ZZ, Liu JW, Zhang Y, Hu XH, Wu GH, Wang HQ, Chen ZC, Chen JC, Zhou QH, Lu JW, Fan QX, Huang JJ, Zheng X. Phase III randomized clinical trial of intratumoral injection of *E1B* gene-deleted adenovirus (H101) combined with cisplatin-based chemotherapy in treating squamous cell cancer of head and neck or esophagus. Ai Zheng 2004; 23:666–1670
- Xiong Y, Hannon GJ, Zhang H, Casso D, Kobayashi R, Beach D. p21 is a universal inhibitor of cyclin kinases. Nature 1993; 366:701–704
- Xu G, Pan J, Martin C, Yeung SC. Angiogenesis inhibition in the in vivo antineoplastic effect of manumycin and paclitaxel against anaplastic thyroid carcinoma. J Clin Endocrinol Metab 2001; 86:1769–77.
- Yang CT, You L, Uematsu K, Yeh CC, McCormick F, Jablons DM. p14ARF modulates the cytolytic effect of ONYX-015 in mesothelioma cells with wild-type p53. Cancer Res 2001; 61:5959–63.
- Yang JC, Haworth L, Sherry RM, Hwu P, Schwartzentruber DJ, Topalian SL, Steinberg SM, Chen HX, Rosenberg SA. A randomized trial of bevacizumab, an anti-VEGF antibody for metastatic renal cancer. N Engl J Med 2003; 349:427–434.

- Yew PR, Berk AJ. Inhibition of p53 transactivation required for transformation by adenovirus early 1B protein. Nature 1992; 357:82–82.
- Yew RP, Lui X, Berk AJ. Adenovirus E1B oncoprotein tethers a transcriptional repression domain to p53. Genes Dev. 1994 ; 8:190–202.
- Yu W, Fang H. Clinical trials with oncolytic adenovirus in China. Curr Cancer Drug Targets. 2007; 2:141-148.
- Zhang ZL, Zou WG, Luo CX, Li BH, Wang JH, Sun LY, Qian QJ *et al*. An armed oncolytic adenovirus system, zd55-gene, demonstrating potent antitumoral efficacy. Cell Res 2003; 13:481−489.

0013-7227/07/$15.00/0
Printed in U.S.A.

Endocrinology 148(11):5186–5194

doi: 10.1210/en.2007-0752

Lovastatin Enhances the Replication of the Oncolytic Adenovirus *dl*1520 and Its Antineoplastic Activity against Anaplastic Thyroid Carcinoma Cells

Silvana Libertini, Irma Iacuzzo, Angelo Ferraro, Mario Vitale, Maurizio Bifulco, Alfredo Fusco, and Giuseppe Portella

Dipartimenti di Biologia e Patologia Cellulare e Molecolare (S.L., I.I., A.Fu., G.P.) and Endocrinologia e Oncologia Molecolare e Clinica (M.V.), and Cattedra di Patologia Clinica (G.P.), Università di Napoli "Federico II," 80131 Napoli, Italy; Naples Oncogenomic Center-Centro Ingegneria Genetica (A.Fe., A.Fu.), Biotecnologie Avanzate, 80145 Naples, Italy; and Dipartimento di Scienze Farmaceutiche (M.B.), Università degli Studi di Salerno, 84084 Naples, Italy

Anaplastic thyroid carcinoma (ATC) is one of the most aggressive solid tumors and shows morphological features of a highly malignant, undifferentiated neoplasm. Patients with ATC have a poor prognosis with a mean survival time of 2–6 months; surgery, radiotherapy, and chemotherapy do not improve survival. Gene therapy approaches and oncolytic viruses have been tested for the treatment of ATC. To enhance the antineoplastic effects of the oncolytic adenovirus *dl*1520 (Onyx-015), we treated ATC cells with lovastatin (3-hydroxymethylglutaryl-CoA reductase inhibitor), a drug used for the treatment of hypercholesterolemia, which has previously been reported to exert growth-inhibitory and apoptotic activity on ATC cells. Lovastatin treatment significantly increased the effects of *dl*1520 against ATC cells. The replication of *dl*1520 in ATC cells was enhanced by lovastatin treatment, and a significant increase of the expression of the early gene *E1A 13 S* and the late gene *Penton* was observed in lovastatin-treated cells. Furthermore, lovastatin treatment significantly enhanced the effects of *dl*1520 against ATC tumor xenografts. Lovastatin treatment could be exploited to increase the efficacy of oncolytic adenoviruses, and further studies are warranted to confirm the feasibility of the approach in ATC patients. (*Endocrinology* 148: 5186–5194, 2007)

THYROID NEOPLASIAS INCLUDE well-differentiated follicular and papillary carcinomas, poorly differentiated papillary and follicular carcinomas, and undifferentiated anaplastic carcinomas (1).

Anaplastic carcinoma (ATC) constitutes 1–7% of all thyroid cancer cases. It arises from thyroid follicular cells showing morphological features of a highly malignant, undifferentiated neoplasm with multiple atypical mitotic figures; it reveals no follicular structures, colloid formation, or other features of thyroid differentiation (2). p53 and β-catenin mutations are the genetic alterations most frequently found in poorly differentiated and anaplastic carcinomas (3).

ATC represents one of the most aggressive human malignancies because it invariably has a fatal prognosis. In fact, the absence of active therapies is the major impediment to the successful control of the disease (2–4). Therefore, novel therapeutic approaches are required.

Selective replication oncolytic viruses represent a novel therapeutic approach; adenovirus and other viruses have been engineered for selective replication within neoplastic cells. The most common approach is the deletion of viral gene whose product is necessary for replication in normal cells but expendable in cancer cells. Unfortunately, due to the multifunctional nature of many viral proteins, the gene deletion approach for viral selective replication frequently results in a reduced replication and therapeutic potency (5).

The first replication-competent adenoviral mutant described, *dl*1520 (Onyx-015), contains a deletion of E1B-55K, which inhibits p53 and prevents apoptosis, allowing *dl*1520 replication in cancer cells lacking functional p53 pathway but not in normal cells. *dl*1520 was expected to replicate selectively in a high percentage of human cancers being the p53 pathway nonfunctional in about 50% of human neoplasia. However, the role of p53 in determining *dl*1520 selectivity has remained controversial for years because it was shown that *dl*1520 can replicate in tumor cell lines retaining wild-type p53 sequences, and its replication in primary cells is not restricted by p53.

Recently it has been shown that E1B-55K mediates late-viral RNA transport, and *dl*1520 tumor-selective replication is determined by a unique property of tumor cells to efficiently export late viral RNA in the absence of E1B-55K. Thus, loss of E1B-55K-mediated late viral RNA export, rather than p53 degradation, is the major determinant of *dl*1520 selective replication in neoplastic cells (5).

The use of *dl*1520 oncolytic virus as monotherapy has demonstrated limitations in efficacy, making more research necessary for the design of strategies that will increase its tumor-eradicating potential (6).

*dl*1520 has been used in conjunction with chemotherapeu-

First Published Online August 9, 2007

Abbreviations: AdGFP, GFP-transducing adenovirus; ATC, anaplastic thyroid carcinoma; CAR, coxsackievirus-adenovirus receptor; Ct, cycle threshold; FACS, fluorescence-activated cell sorter; FITC, fluorescein isothiocyanate; GFP, green fluorescent protein; HEK, human embryonic kidney; MEK, MAPK kinase; MOI, multiplicity of infection; pfu, plaque-forming unit.

***Endocrinology* is published monthly by The Endocrine Society (http://www.endo-society.org), the foremost professional society serving the endocrine community.**

tic agents in clinical trials with evidence for potential synergistic antitumor activity. The use of *dl*1520 in conjunction with cisplatin and 5-fluorouracil has been examined in a phase II clinical trial involving head and neck carcinoma patients. *dl*1520 has been used in combination with leucovorin and 5-fluorouracil in a phase II trial in patients with gastrointestinal carcinoma metastatic to the liver and with gemcitabine in a phase I/II trial in patients with unresectable pancreatic carcinoma (6, 7). All these studies have shown that combined treatment with *dl*1520 and chemotherapy increases the therapeutic effects.

We previously demonstrated an antineoplastic activity of *dl*1520 against ATC cell lines; however, high multiplicity of infections (MOIs) were used (8). Synergistic cell killing effects of *dl*1520 with doxorubicin or paclitaxel were observed in ATC cell lines, with the IC_{50} drug values reduced 1.75- to 11-fold in the presence of *dl*1520 (8). We have also shown increased efficacy of *dl*1520 followed by ionizing radiations, compared with either treatment alone (9). These data, previously obtained by us, suggest that *dl*1520 may be a valid tool in the treatment of anaplastic thyroid carcinoma in combination with other agents.

To develop novel therapeutic strategies based on replication selective adenoviruses, it is important to identify drugs able to enhance the oncolytic activity. In the present study, we evaluated the effects of lovastatin in combination with *dl*1520 against ATC cells.

Lovastatin (3-hydroxy-methylglutaryl-CoA reductase inhibitor), a drug used for the treatment of hypercholesterolemia, has been reported to exert growth-inhibitory activity *in vitro* and *in vivo*. Farnesyl- and geranylgeranylpyrophosphate, intermediates in the cholesterol synthetic pathway, are needed for isoprenylation, a crucial step for membrane attachment of cellular proteins like Ras, Rho, Cdc42, Rac, *etc.* (10, 11). By inhibiting protein isoprenylation, lovastatin induces a reduction of cell proliferation and apoptosis (10–11). Moreover, it has been demonstrated that low doses of lovastatin induce apoptosis of ATC cells (12, 13).

We have observed that lovastatin significantly enhanced the antineoplastic activity of *dl*1520 against ATC cells and its replication. Furthermore, a significant increase in viral gene expression was induced by lovastatin in ATC cells. Finally, the combined treatment induced a significant reduction of the growth of ATC tumor xenografts.

Materials and Methods

Cell lines and preparation of adenoviruses

The human anaplastic thyroid carcinoma cell lines used in the study are ARO, FRO, KAT-4, and Cal 62.

ARO and FRO human thyroid anaplastic carcinoma cell lines were established by Dr. G. J. Juillard (Department of Radiation Oncology, University of California, Los Angeles, Los Angeles, CA), and ARO and FRO cell lines were kindly provided by Professor J. A. Fagin (University of Cincinnati College of Medicine, Cincinnati, OH). KAT-4 cells were obtained from Dr. Ain (University of Kentucky, Lexington, KY). Cal 62 cell line was obtained from Deutsche Sammlung von Mikroorganismen und Zellkulturen GmbH (Braunschweig, Germany), German Collection of Microorganisms and Cell Cultures.

The NPA line derives from poorly differentiated papillary carcinoma and was obtained by Dr. G. J. Juillard. The FB1 cell line derives from a follicular carcinoma (14). Human embryonic kidney (HEK)-293 cells were obtained from American Type Culture Collection (Manassas, VA).

KAT-4 cells harbor a mutated *p53* gene, (273 Arg->His), whereas FRO cells express very low levels of p53, but no *p53* gene mutation was observed (8).

Cells were grown in DMEM supplemented with 10% fetal calf serum, glutamine, and ampicillin/streptomycin.

*dl*1520 (ONYX-015), a gift from Dr. A. Balmain (Cancer Research Institute, University of California, San Francisco, CA) and Dr. I. Ganly (Memorial Sloan-Kettering Cancer Center, New York, NY), is a chimeric human group C adenovirus (Ad2 and Ad5) that has a deletion between nucleotides 2496 and 3323 in the E1B region that encodes the 55-kDa protein. In addition, there is a C to T transition at position 2022 in region E1B that generates a stop codon at the third codon of the protein. Viral stocks were expanded in the HEK-293 cell line and purified, as previously reported (8).

Stocks were stored at −70 C after the addition of glycerol to a concentration of 50% (vol/vol). Virus titer was determined by plaque-forming units (pfu) on the HEK-293 cells.

Adenovirus infection

Cells were detached, counted, and plated in 6-well plate at 70% cell density. After 24 h, cells were infected with a green fluorescent protein (GFP)-transducing adenovirus (AdGFP), a nonreplicating E1 and E2-deleted adenovirus encoding GFP, diluted in growth medium at different MOIs; medium was replaced after 2 h. Cells were washed 24 h after infection and then trypsinized, washed, and resuspended in 300 μl PBS and analyzed for GFP expression on a fluorescence-activated cell sorter (FACS) cytometer (Dako Cytomation, Carpinteria, CA) and Summit version 4.3 software (Dako, Carpinteria, CA).

Different treatment conditions were used for the evaluation of lovastatin effects: antineoplastic effects were evaluated in the presence of lovastatin, whereas experiments designed to evaluate the effects of the drug on the early phases of viral infection were performed with a short treatment time.

For the evaluation of lovastatin effects on adenoviral entry and GFP expression, the cells were treated for 16 h with 10 μM lovastatin and then infected for 24 h with AdGFP. Cells were harvested and prepared for FACS analysis as previously described.

For the evaluation of the cytoxic effects of the *dl*1520 virus, 1×10^3 cells were seeded in 96-well plates, and 24 h later lovastatin was added to the incubation medium. After an additional 16 h, medium was replaced with a medium containing or not lovastatin plus *dl*1520 at different MOIs. After 14 d the cells were fixed with 10% trichloroacetic acid and stained with 0.4% sulforhodamine B in 1% acetic acid (15). The bound dye was solubilized in 200 μl of 10 mM unbuffered Tris solution, and the optical density was determined at 490 nm in a microplate reader (Bio-Rad Laboratories, München, Germany). The percent of survival rates of treated cells were calculated by assuming the survival rate of untreated cells to be 100%.

Quantitative PCR of dl1520

To quantify the amount of *dl*1520 virus genome on lovastatin treatment, ATC cells were treated with 10 μM lovastatin for 16 h and then media replaced with a medium containing different MOIs of *dl*1520 alone or with lovastatin. After 24 h of infection, cell media were collected and viral DNA extracted using a QIAamp DNA minikit (QIAGEN, Valencia, CA). Viral DNA was then quantified by real-time PCR using assay-specific primer and probe. A real-time-based assay was developed using the following primers: 5′-GCCACCGAGACGTACTTCAGC-CTG-3′ (upstream primer) and 5′-TTG TAC GAG TAC GC G GTA TCCT-3′ (downstream primer) for the amplification of 143 bp sequence of the viral hexon gene (from bp 99 to 242 bp). For quantification, a standard curve was constructed by assaying serial dilutions of *dl*1520 virus ranging from 0.1 to 100 pfu.

To quantify the amount of *dl*1520 virus genome in tumor xenografts, total DNA was extracted from 20 mg of each sample using a DNA purification system (Promega Corp., Madison, WI). DNA was resuspended in 200 μl of water and 2 μl used for the real-time PCR-based assay. For each experiment the DNA was extracted from three different samples of each treatment group.

Quantitative RT-PCR of dl1520 gene expression

Cells were infected with 10 or 100 pfu of *dl*1520, in the presence or in the absence of 10 μM of lovastatin, and harvested at 24 h after infection. Cells were dissolved in 1 ml Trizol (Invitrogen, Carlsbad, CA). RNA quality was evaluated by agarose gel electrophoresis; DNase treatment was performed. One microgram of total RNA was reverse transcribed and the expression of *E1A 13 S* and *Penton* genes monitored using real-time PCR with the following specific primers: E1A 13 S forward, 5′-AATGGCCGCCAGTCTTTT-3′ and reverse, 5′-ACACAGGACTG-TAGACAA-3′; Penton forward, 5′-TAACCAGTCACAGTCGCAAG-3′ and reverse, 5′-CCCGCGCCTTAAACTTATT-3′ (16). To calculate the relative expression levels, we used the $2^{-[\Delta][\Delta]}$cycle threshold (Ct) method. Negative controls, samples without RT-PCR, or CDNA template were included in every PCR run, always resulting negative (data not shown).

Detection of cell surface coxsackievirus-adenovirus receptor (CAR) receptor

Cells were grown in six-well plates. After 48 h cells were detached in PBS-EDTA 10 mM, washed with PBS, and then incubated 1.5 h in FACS buffer with a mouse anti-CAR monoclonal antibody RmcB (1:250) (17). After washing, the cells were incubated in FACS buffer containing the secondary antibody conjugated to fluorescein isothiocyanate (FITC) (1: 100; Sigma, St. Louis, MO) and analyzed for CAR expression on a Cyan cytometer (Dako Cytomation) and Summit version 4.3 software (Dako).

Human thyroid tissue samples and real time RT-PCR

Normal and neoplastic human thyroid tissues were obtained from surgical specimens and immediately frozen in liquid nitrogen. Thyroid tumors were collected at the Laboratoire d'Histologie et de Cytologie, Centre Hospitalier (Lyon Sud, France) and the Laboratoire d'Anatomie Pathologique, Hospital de L'Antiquaille (Lyon, France).

Total RNA was isolated and DNase digested using the RNeasy mini-kit (QIAGEN) according to the manufacturer's recommendations. One microgram of total RNA from each sample was reverse transcribed using random hexamers as primers and Moloney leukemia virus reverse transcriptase (Applied Biosystems, Foster City, CA) to yield cDNA.

To design a quantitative PCR assay, a human ProbeLibray system (Exiqon, Vedbaek, Denmark) was used. Probe and primers pair to amplify a fragment for real-time PCR of Cxadr mRNA were selected entering its accession number (NM001338.3) on the assay design page of the ProbeFinder software. ProbeFinder generated an intron-spanning assay identifying the exon-exon boundaries within submitted transcript. An amplicon of 93 nucleotides scattered among sixth and seventh exon was selected. The primer sequences were: Cxadr forward, 5′-AT-GAAAAGGAAGTTCATCAACGTA-3′, Cxadr reverse, 5′-AATGAT-TACTGCCGATGTAGCTT-3′. The same procedure was used to select probe and primes for housekeeping gene G6PDH, accession no. X03674. The primer sequences were: G6PDH forward, 5′-ACAGAGTGAGC-CCTTCTTCAA-3′, G6PDH reverse, 5′-GGAGGCTGCATCATCGTACT-3′. All fluorigenic probes were dual labeled with FAM at 5′end and with a black quencer at the 3′end.

Relative quantitative TaqMan RT-PCR was performed in a Chromo4 detector (MJ Research, Waltham, MA) in 96-well plates using a final volume of 25 μl. The conditions used for PCR were 10 min at 95 C and then 45 cycles of 20 sec at 95 C and 1 min at 60 C. Each reaction was performed in duplicate. To calculate the relative expression levels, we used the $2^{-[\Delta][\Delta]Ct}$ method, where $[\Delta][\Delta]C_t = [\Delta]C_{t,sample} - [\Delta]C_{t,reference.}$

Written informed consent was obtained from all participants. The study protocol was approved by the ethics committees of the Centre Hospitalier Lyon Sud and the University Federico II, Napoli, and conducted in accordance with the principles of the Declaration of Helsinki as revised in 2000.

Protein extraction and Western blot analysis

In all experiments 70% confluent cells were used. Cells were homogenized directly into lysis buffer (50 mM HEPES, 150 mM NaCl, 1 mM EDTA, 1 mM EGTA, 10% glycerol, 1% Triton X-100, 1 mM phenylmethylsulfonyl fluoride, 1 μg/ml aprotinin, 0.5 mM sodium orthovanadate, 20 mM sodium pyrophosphate). The lysates were clarified by 20 min centrifugation at 14,000 $\times$ *g*. Protein concentrations were estimated by a Bio-Rad assay, and then proteins were boiled in Laemmli buffer [Tris-HCl (pH 6.8) 0.125 M, sodium dodecyl sulfate 4%, glycerol 20%, 2-mercaptoethanol 10%, bromophenol blue 0.002%] for 5 min before electrophoresis. Proteins were subjected to SDS-PAGE (10% polyacrylamide) under reducing conditions. After electrophoresis, proteins were transferred to nitrocellulose membranes (Immobilon; Millipore Corp., Billerica, MA); complete transfer was assessed using prestained protein standards (Bio-Rad, Hercules, CA). After blocking with Tris-buffered saline-BSA [25 mM Tris (pH 7.4), 200 mM NaCl, 5% BSA], the membrane was incubated with the primary polyclonal rabbit antibody (Santa Cruz Biotechnology, Santa Cruz, CA) against CAR receptor SC-15–405 (1:200) for 1 h (at room temperature) or with the monoclonal antibody against against β-actin (Sigma). Membranes were then incubated with the horseradish peroxidase-conjugated secondary antibody (1:10,000) for 45 min (at room temperature), and the reaction was detected with an ECL system (Amersham Life Science, Buckinghamshire, UK).

Tumorigenicity assay

Experiments were performed with 6-wk-old female athymic mice (Charles River, Calco, Lecco, Italy). FRO cells (4×10^6) were injected into the right flank of 80 athymic mice. After 20 d, when tumors were clearly detectable, the animals were divided into four groups (20 animals/group), and tumor volume was evaluated. Two groups received lovastatin in the drinking water (40 mg/1000 ml) and after 6 d *dl*1520 (5×10^7 pfu) was injected in the peritumoral area in a group treated with lovastatin and in an untreated group.

Tumor diameters were measured with calipers every second day by two blind and neutral observers until the animals were killed. No mouse showed signs of wasting or other indications of toxicity. Tumor volumes were calculated by the formula of rotational ellipsoid: Tumor volume = $A \times B^2/2$, where A is the axial diameter and B is the rotational diameter.

All mice were maintained at the Dipartimento di Biologia e Patologia Cellulare e Molecolare Animal Facility. The animal experimentations described herein were conducted in accordance with accepted standards of animal care and in accordance with the Italian regulations for the welfare of animals used in studies of experimental neoplasia, and the study was approved by our institutional committee on animal care.

The amount of lovastatin administered was chosen considering that the average daily water intake for each mouse was 5–7.5 ml and 10 mg/kg/d was the best dose of lovastatin for obtaining biological effects in mice.

To evaluate the genome equivalent copies of *dl*1520 in tumor xenografts, three animals bearing FRO xenografts received lovastatin in the drinking water (40 mg per 1000 ml). After 6 d, *dl*1520 (5×10^7 pfu) was injected in the peritumoral area of the mice treated with lovastatin and in three untreated mice.

After 48 h animals were killed, tumors excised, DNA extracted, and viral replication evaluated by real-time PCR. DNA quality was analyzed by real-time PCR of the β-actin gene.

Statistical analysis

Comparisons among different treatment groups in the experiments *in vivo* were made by the ANOVA method and the Bonferroni *post hoc* test using a commercial software (Prism 4; GraphPad, San Diego, CA). Assessment of differences among rate of tumor growth in mice was made for each time point of the observation period; treatment groups were control, *dl*1520, lovastatin, and lovastatin plus *dl*1520.

The analysis of the cell-killing effect *in vitro* was also made by the ANOVA method and the Bonferroni *post hoc* test. For all the other experiments, comparisons among groups were made by the ANOVA method and *t* test.

Results

Analysis of adenoviral infectivity of human thyroid carcinoma cell lines

To evaluate the susceptibility of ATC cells to adenoviral infection, we infected a panel of thyroid carcinoma cell lines using an AdGFP; the results are shown in Fig. 1A.

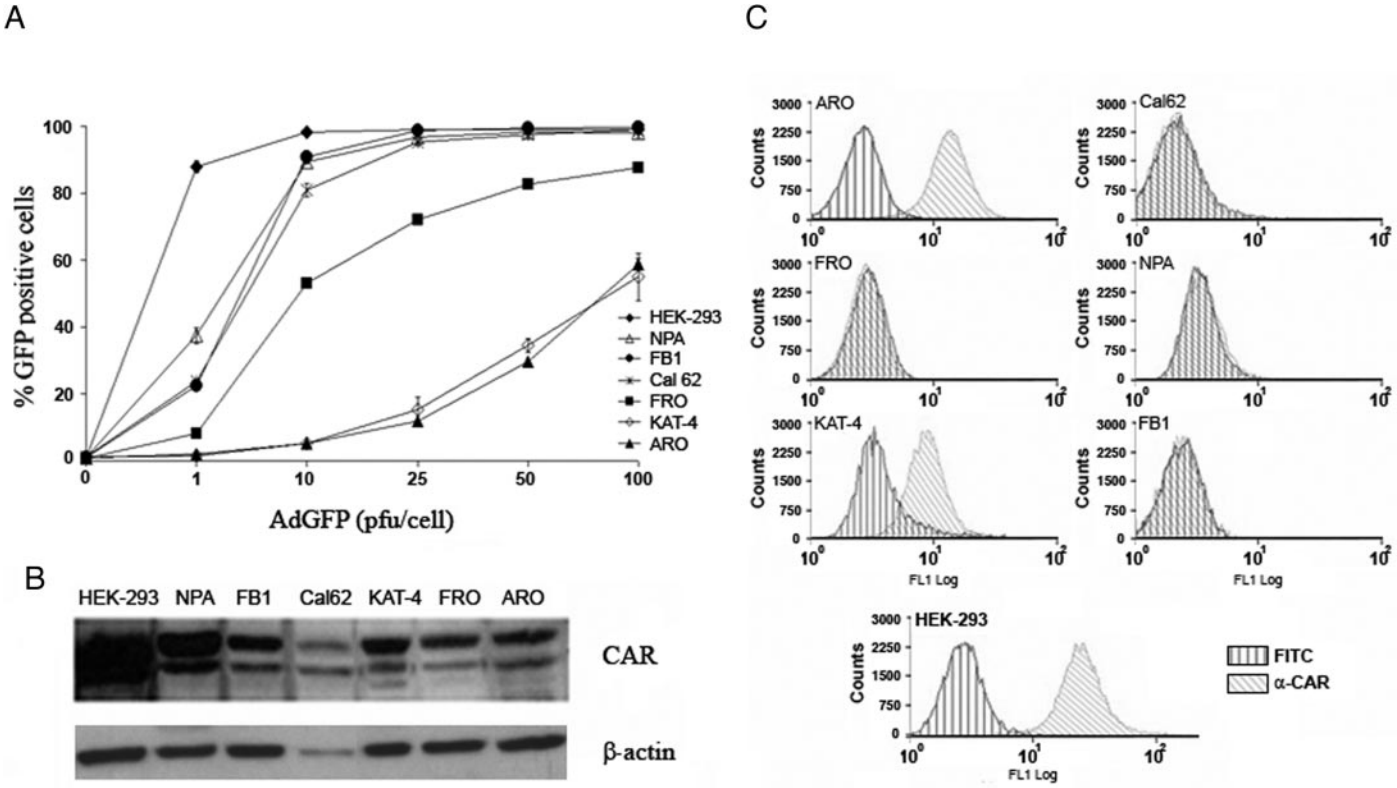

FIG. 1. A, Percentage of positive cells upon AdGFP infection. Cells were infected at different MOIs with AdGFP, and after 24 h the percentage of fluorescent cells was evaluated by FACS analysis. ATC cell lines ARO and KAT-4 were the less sensitive to AdGFP infection at all MOIs used, whereas FRO and Cal 62 cells displayed a higher percentage of GFP-expressing cells. FRO cells showed about 50% of GFP-positive cells at 10 MOI; conversely, Cal 62 at the same MOI showed about 80% of positive cells. Follicular thyroid carcinoma cell line FB1 and papillary thyroid carcinoma cell line NPA showed about 90% of GFP-positive cells at 10 MOI. HEK-293 cells were used as a positive control. The data are the mean of three different experiments; the *bar* represents the SD. B, Western blot analysis of CAR expression in thyroid carcinoma cell lines. Cal 62, FRO, and ARO cells showed low expression of total CAR levels, whereas FB1, KAT-4, and NPA cells expressed the higher of total CAR levels. Equal amounts of protein lysates (50 μg) were loaded. C, Cytofluorimetric analysis of CAR expression on the membrane of thyroid carcinoma cell lines. Flow cytometry analysis showed the absence of cell surface CAR expression in FRO, NPA, Cal 62, and FB1 thyroid cancer cell lines. ARO and KAT-4 cell lines showed the presence of CAR on the membrane. HEK-293 cells were used as positive control. Cells were incubated with a anti-CAR (RmcB) monoclonal antibody or FITC-labeled mouse alone. In all experiments, 70% confluent cells were used.

The anaplastic thyroid carcinoma cell lines ARO, FRO, and KAT-4 display the lowest percentage of fluorescent cells at all the MOIs used; indeed 100 pfu/cell are required to obtain greater than 50% ARO- and KAT-4-positive cells, whereas at 10 pfu/cell, about 50% of FRO cells are positive. Conversely, follicular thyroid carcinoma cell line FB1 and papillary thyroid carcinoma cell line NPA showed about 90% of GFP-positive cells at 10 MOI. As a positive control HEK-293 cells were used.

Because adenoviral infection occurs via the attachment to the CAR (18), we analyzed CAR expression by Western blot; two CAR-specific bands of 44 and 46 kDa, respectively, were detected in all the samples (Fig. 1B). However, certain differences were observed in their levels; in ATC cell lines, variable levels ranging from very low to intermediate were observed; the papillary thyroid carcinoma-derived NPA cell line, the follicular carcinoma-derived FB-1 cell lines, and the ATC-derived KAT-4 cell line express the highest CAR levels. A cytofluorimetric analysis was performed to evaluate the presence of CAR on the cell membrane (Fig. 1C), showing the absence of CAR on the cell surface in FRO, NPA, Cal 62, and FB1 cells. This observation suggests a CAR-independent entry of AdGFP in these cell lines. The cell lines ARO and KAT-4 showed the presence of CAR on the cell membrane despite being the less susceptible to adenoviral infection.

To confirm that anaplastic thyroid carcinomas express low levels of CAR, we evaluated the CAR mRNA levels in human thyroid carcinoma tissues by RT-PCR. Significantly lower levels (**, $P < 0.01$) in CAR gene expression were observed in papillary carcinomas, follicular carcinomas, and anaplastic thyroid carcinomas with respect to normal thyroid samples (Fig. 2).

Lovastatin enhances the cell killing effects and the replication of the oncolytic adenovirus dl1520

Because our data show that ATC are not readily infected by therapeutic adenoviruses, we decided to evaluate the effects of lovastatin in combination with *dl*1520. KAT-4 cells were chosen as representative of ATC cells at low sensitivity to the infection with *dl*1520; the FRO cell line was chosen as representative of an intermediate infectivity (8, 9).

In both cell lines, the combined treatment enhanced the cell-killing activity of *dl*1520. In FRO cells treated with 10 pfu/cell of *dl*1520, an additive and significant (2.5 μM) and

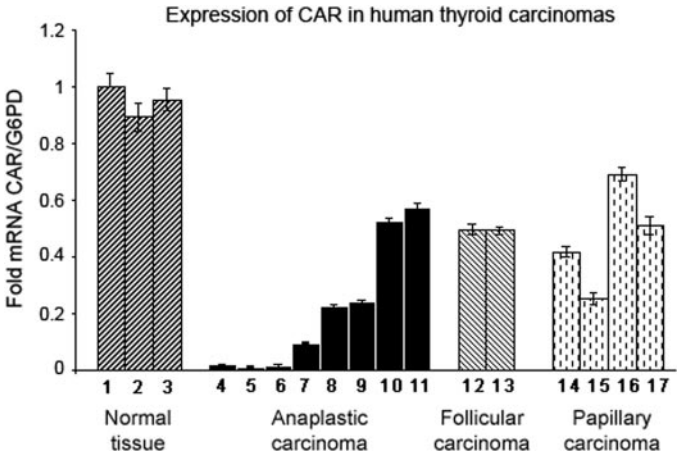

FIG. 2. CAR expression in thyroid carcinoma tissues. Three normal thyroid samples (1–3), eight anaplastic (4–11), two follicular (12 and 13), and four papillary (14–17) thyroid carcinomas were used for real-time RT-PCR analysis of CAR expression, showing a reduction in CAR mRNA levels in all neoplastic tissues with respect to normal thyroid samples.

highly significant (5 μM) increase in cell killing was observed. In KAT-4 cells a highly significant increase in cell killing was induced by lovastatin treatment at all MOIs and lovastatin concentrations used (Fig. 3A).

Next, we quantified the amount of *dl*1520 virus genome by real-time PCR in FRO and KAT-4 cells untreated, treated with lovastatin for 16 h (lovastatin 16 h) before infection, or kept in the presence of lovastatin after the infection (lovastatin) and infected with different MOIs. In FRO cells at 10 pfu/cell, both lovastatin treatments induced an highly significant (**, $P < 0.01$) increase in viral replication (Fig. 3B). KAT-4 cells kept in the presence of lovastatin also showed a highly significant increase in viral replication (**, $P < 0.01$), whereas 16 h treatment did not modify viral replication.

Lovastatin enhances the expression of viral genes

Because ATC cells infected in the presence of lovastatin show an increase in viral replication, we decided to evaluate the infectivity of ATC cells in the presence of lovastatin. KAT-4 and FRO cells were pretreated with a noncytotoxic concentration of lovastatin (10 μM) for 16 h and then infected with AdGFP at different MOIs. FACS analysis of treated or untreated cells showed that lovastatin treatment induced a highly statistically significant (**, $P < 0.01$) increase in the number positive cells ranging from 3 up to 10% (Fig. 4A).

Both cell lines showed a strong increase in fluorescence to cell ratio on lovastatin treatment (Fig. 4A).

Pharmacological inhibitors of the Raf-MAPK kinase (MEK)-ERK pathway up-regulates CAR expression on the cell surface of cancer cells (19); lovastatin is a well-known inhibitor of p21 Ras isoprenylation and activity. Therefore, we evaluated the effects of lovastatin on CAR expression in

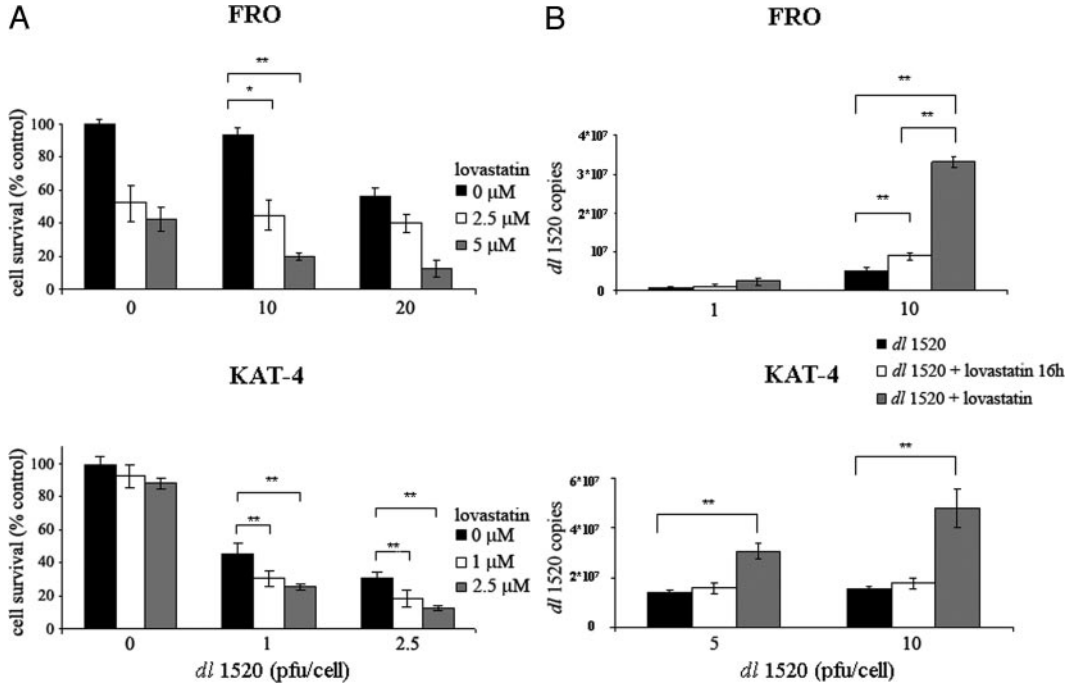

FIG. 3. A, Lovastatin treatment enhances the cell-killing effects of the oncolytic adenovirus *dl*1520. FRO and KAT-4 cells were treated with lovastatin and then infected with the oncolytic adenovirus *dl*1520 at different MOIs. In FRO cells kept in the presence of lovastatin, a highly significant increase (**, $P < 0.01$) in the cell-killing activity of 10 pfu/cell of *dl*1520 was observed in association with 5 μM of lovastatin. In KAT-4 cells kept in the presence of 1 and 2.5 μM of lovastatin, a highly significant increase (**, $P < 0.01$) of the cell-killing activity in combination with 1 and 2.5 pfu/cell of *dl*1520 was obtained. Viral concentration able to induce the same cell-killing in the two cell lines were used. The data are expressed as percentages of untreated control cells and are the mean of five different experiments; the *bar* represents the SD. B, Lovastatin treatment enhances the replication of the oncolytic adenovirus *dl*1520. FRO and KAT-4 cells were treated with lovastatin (10 μM) for 16 h and then infected with a medium containing *dl*1520 (lovastatin 16 h) or *dl*1520 plus lovastatin (lovastatin). FRO cells at 10 pfu/cell showed a highly significant increase (**, $P < 0.01$) of *dl*1520 replication in both groups. KAT-4 cells at 5 and 10 pfu/cell showed a highly significant increase (**, $P < 0.01$) of *dl*1520 replication only in the group kept in the presence of lovastatin. The data are the mean of three different experiments; the *bar* represents the SD.

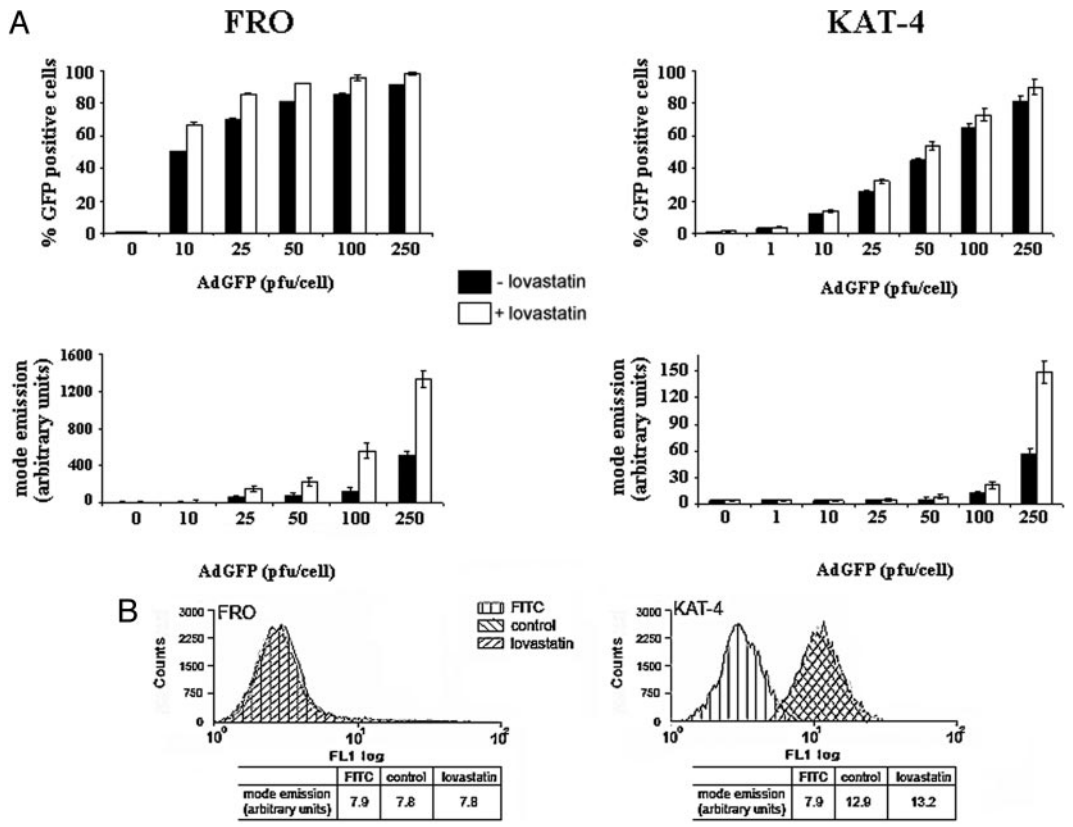

FIG. 4. A, Percentage of GFP-positive cells and fluorescence to cell ratio in lovastatin-treated cells. FRO and KAT-4 cells were treated with 10 μM of lovastatin for 16 h and then infected with AdGFP at different MOIs. FACS analysis was performed 24 h after the infection. Lovastatin increased the percentage of AdGFP-positive KAT-4 and FRO cells (*upper panel*). Highly significant difference between treated and untreated cells is observed in both cell lines starting from 10 pfu/cell point. Lovastatin-treated cells showed an increase in fluorescence to cell ratio (*lower panel*). The difference is statistically high ($P < 0.01$), starting from 25 pfu/cell (FRO cells) or 50 pfu/cell (KAT-4 cells).The data are the mean of five different experiments; the *bar* represents the SD. B, Lovastatin does not modify CAR expression on the cell surface of KAT-4 and FRO cells. KAT-4 and FRO cells were treated with 10 μM lovastatin for 16 h and then incubated with anti-CAR (RmcB) monoclonal antibody (lovastatin) and compared with untreated control cells (control). Background emission was assessed by incubating KAT-4 and FRO cells with FITC-labeled mouse alone (FITC). CAR expression was not modified by lovastatin treatment. The data are representative of three different experiments.

ATC cells. CAR levels on cell surface, evaluated by FACS analysis (Fig. 4B), were not modified by lovastatin treatment.

Because lovastatin-treated cells showed an increased in fluorescence to cell ratio, we hypothesized that lovastatin treatment could enhance viral gene expression. To monitor the expression of adenoviral genes in lovastatin-treated ATC cells we selected two adenoviral genes, whose expression is correlated with different stages of the adenoviral life-cycle: *E1A 13 S* representing genes transcribed from the immediate early region and *Penton* representing genes expressed from the late region.

FRO and KAT-4 cells were infected respectively with a MOI of 100 and 10 pfu of dl1520 in the presence or in the absence of lovastatin (10 μM). The expression levels of E1A 13 S and *Penton* gene were measured by real-time RT-PCR at 24 h. Cotreatment with lovastatin significantly (*, $P < 0.05$) enhanced the expression levels of *E1A 13 S* and *Penton* gene in both cell lines (Fig. 5).

Lovastatin in combination with dl1520 reduces the growth of ATC tumor xenografts

To demonstrate that the combined treatment lovastatin and *dl*1520 could potentially yield improved clinical efficacy, we evaluated the effects of lovastatin treatment *in vivo*.

FRO cells were injected into the right flank of athymic mice, and after 20 d, when tumors were clearly detectable (T = 0), animals were randomized into four groups and lovastatin was added in the drinking water of two groups. The animals received lovastatin until the end of the experiment. After 6 d *dl*1520 was injected within the tumor (T = 6), twice per week. In Fig. 6A, tumor growth is expressed as a percentage of growth relative to the volume observed at T = 0.

*dl*1520 treatment was able to significantly reduce (*, $P < 0.05$) the growth of tumor xenografts in the initial phase of the treatment (up to T = 30). Conversely, the combination lovastatin plus *dl*1520 was able to induce a highly significant reduction (**, $P < 0.01$) in tumor growth until the end of experiment, confirming that lovastatin enhances the antineoplastic effects of *dl*1520. No toxicities were observed in treated animals.

Finally, we evaluated by real-time PCR (Fig. 6B) the genome equivalent copies of *dl*1520 in animals bearing FRO xenografts and treated with *dl*1520 and *dl*1520 plus lovastatin. Lovastatin treatment was able to induce a 10-fold increase in viral replication.

Discussion

ATC represents one of the most lethal human neoplasia being refractory to conventional therapies, including sur-

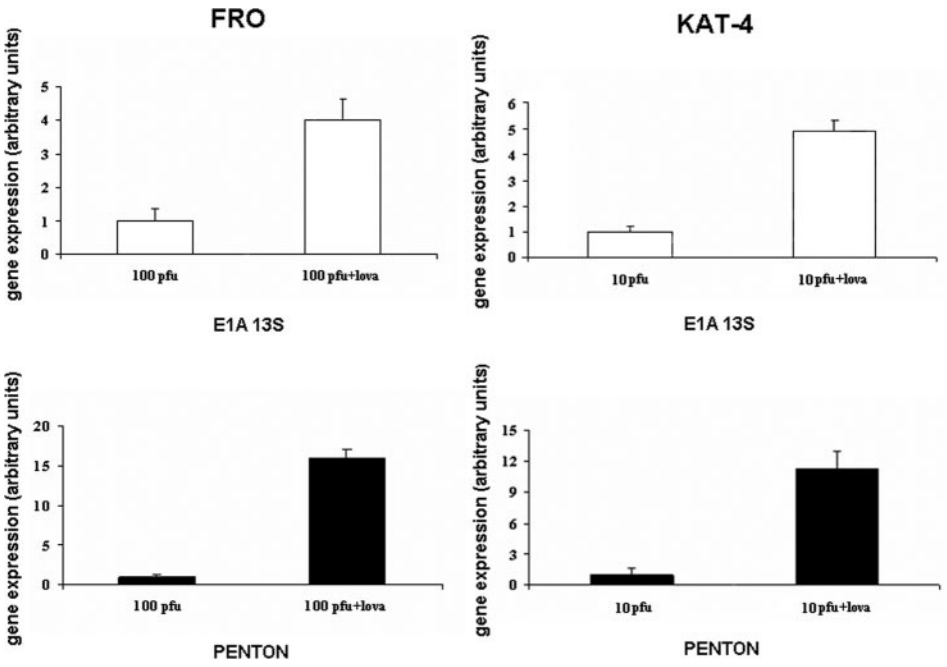

FIG. 5. Lovastatin increases viral gene expression in ATC cells. FRO and KAT-4 cells were treated with 10 μM of lovastatin; after 16 h cells were infected with *dl*1520. For FRO cells a MOI of 100 pfu was used; KAT-4 cells were infected with 10 pfu. After 24 h the levels of expression of the adenoviral immediate early region gene *E1A 13 S* and the adenoviral of late region gene *Penton* were measured by real-time RT-PCR. Lovastatin treatment significantly enhanced the expression levels of the *E1A 13 S* and Penton gene. In FRO cells a 4-fold increase of *E1A 13 S* expression levels and 16-fold increase of Penton gene were obtained. In KAT-4 cells, a 5-fold increase of *E1A 13 S* expression levels and 12-fold increase in Penton expression levels were observed. The data are the mean of three different experiments; the *bar* represents the SD.

gery, radioactive iodine, and chemotherapy (2–4). Development and evaluation of novel treatment strategies are needed.

Replication-selective oncolytic viruses (virotherapy) are being developed as a novel, targeted form of anticancer treatment. *dl*1520 (Onyx-015) was the first virus that had been genetically engineered for replication-selectivity for treatment in cancer patients. Recent results from a phase III clinical trial have confirmed the ability of an oncolytic adenovirus (H101) bearing an E1B-55kD gene deletion similar to that present in *dl*1520 to increase the response rate of nasopharyngeal carcinoma in combination with cisplatin (20).

Selective oncolytic replicating adenoviruses have been tested in ATC cell lines and tumor xenografts showing promising results (8, 9); however, high MOIs of *dl*1520 were required to efficiently kill ATC cells.

The efficacy of oncolytic adenoviruses as therapeutic agents relies on the capability of target neoplastic cells to bind, internalize, and sustain the replication of adenoviruses. We analyzed the infectivity of a panel of human thyroid carcinoma cell lines, showing a low infectivity in most ATC cell lines. Conversely, papillary or follicular thyroid carcinoma cells display a higher infectivity. In a previous study, we evaluated the infectivity of ATC cell lines ARO, KAT-4, and FRO infecting the cells for 48 h with a *lac*Z-transducing adenovirus and evaluating the percentage of infected cells counting stained cells in randomly selected fields. The different results obtained in the two studies can be explained with the use of different reporter genes, infection times, and detection techniques.

Adenovirus internalization relies on the presence of cell surface of the CAR; a Western blot analysis has been performed on total cell lysates showing discrete or high expression levels of CAR. However, cytofluorimetric assay for CAR expression on cell surface showed a low or absent expression of CAR, suggesting a CAR-independent adenoviral entry in thyroid carcinoma cells lines. Furthermore, a significant reduction in CAR gene expression was observed in anaplastic

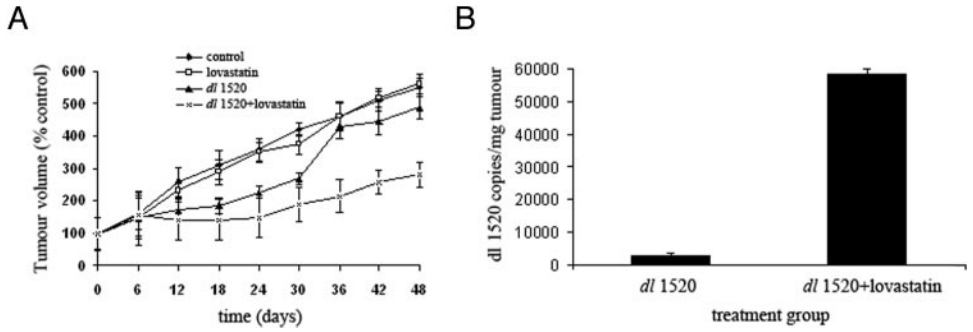

FIG. 6. Tumor growth delay induced by lovastatin and *dl*1520. A, Relative tumor growth of animals treated with *dl*1520 and lovastatin and control groups. Lovastatin treatment alone did not show statistically significant differences with the untreated control, whereas *dl*1520 induced a statistically significant reduction ($P < 0.05$) in the initial phase of the treatment (up to T = 30). The combination of *dl*1520 plus lovastatin significantly delayed tumor growth, compared with *dl*1520 single treatment group from T = 36 ($P < 0.01$). Data are presented as mean ± SD. B, Genome equivalent copies in tumor xenografts. A 10-fold increase in genome equivalent copies in tumor xenografts excised from lovastatin plus *dl*1520 group was observed. The data are the mean of three different experiments; the *bar* represents the SD.

thyroid carcinomas samples, compared with normal thyroid tissues.

Our observations are in agreement with previous studies and confirm a low susceptibility of ATC cells to therapeutic approaches based on adenoviral vectors (21).

It is worth noting that CAR expression is negatively regulated by TGF-β during the switch from epithelial to mesenchymal phenotype, and human pancreatic carcinoma cells show loss of epithelial differentiation and CAR surface localization on TGF-β treatment (22). In ATC cell lines, we observed discrete or high total expression levels of CAR and loss of surface localization of CAR. Our results indicate that the loss of thyroid differentiation, a typical feature of ATC, causes an intracellular localization of CAR receptor, probably by increasing the recycling of CAR receptors or shifting them to the cytosol.

Because ATC cells display a low infectivity and a high MOI of *dl*1520 is required to efficiently kill these cells, we decided to enhance the oncolytic activity by using lovastatin in combination with *dl*1520.

Lovastatin, a drug used for the treatment of hypercholesterolemia, has previously been reported to exert growth-inhibitory activity *in vitro* and *in vivo*. Farnesyl- and geranylgeranylpyrophosphate, intermediates in the cholesterol synthetic pathway, are needed for isoprenylation a crucial step for membrane attachment of cellular proteins like of p21 Ras, Rho, Cdc42, Rac, *etc.* (10). By inhibiting protein isoprenylation, lovastatin exerts its cellular effects, including a reduction of cell proliferation and induction of apoptosis (10). It is worth noting that low doses of lovastatin induce apoptosis or differentiation of ATC cells (11, 12).

Our study demonstrates that the treatment of ATC cell lines KAT-4 and FRO with lovastatin significantly increased the effects of *dl*1520.

A significant increase in viral replication was observed in lovastatin-treated cells. In FRO cells a significant increase was observed infecting lovastatin-treated cells with 10 pfu/cell, whereas at 1 pfu/cell, no significant differences were observed. In KAT-4 cells kept in the presence of lovastatin and infected with 5 or 10 pfu/cell, significant increase was observed; however, the pretreatment with lovastatin for 16 h was not able to increase viral replication.

These results suggest that the increase in viral replication observed treating ATC cells with lovastatin is viral dose or lovastatin treatment time dependent. Therefore, it is possible that higher MOIs of *dl*1520 in combination with a 16-h lovastatin pretreatment could result in enhanced viral replication in KAT-4 cells.

Increased infection efficacy could account for the increased oncolytic activity after lovastatin treatment; moreover, lovastatin inhibits the isoprenylation and the activity of p21 ras, blocking MEK activity, and it has been reported that MEK inhibitors, U0126 and PD184352, increase the expression of CAR protein and adenoviral entry in cancer cells (19). Therefore, we evaluated the adenoviral entry and CAR expression levels in ATC cell lines treated with lovastatin. We observed a modest, albeit significant, increase in adenoviral entry (3–10%), which that it is not sufficient to explain the effects of lovastatin on viral replication and cell survival.

CAR expression levels either total (data not shown) or on the cell surface were not modified by lovastatin treatment.

Cholesterol deprivation of FRO and KAT-4 cells did not modify adenoviral entry (data not shown), suggesting that the effects of lovastatin were not mediated by the inhibition of cholesterol synthesis.

It has been shown that lovastatin inhibits the invasiveness of an ATC cell line (ARO) and focal adhesion kinase phosphorylation, a nonreceptor tyrosine kinase playing a crucial role in integrin-mediated cell adhesion (23); therefore, it is not possible to exclude that lovastatin induces changes in integrin pattern on cell surface. Because it has been suggested that integrins can act as a coreceptor for adenovirus types 2 and 5 (24), the modest increase in adenoviral entry observed by us could be due to changes in integrins pattern induced by lovastatin. Further studies are required to verify this hypothesis.

A high increase in the fluorescence to cell ratio of lovastatin-treated cells was observed. This observation suggested to us that the drug could enhance the expression of viral genes, thereby increasing viral replication. To confirm this hypothesis, the expression of two viral genes, representing the early and the late phases, was analyzed in ATC cells infected with *dl*1520. Lovastatin increased significantly the expression of early gene *E1A 13 S* and a late gene *Penton*.

It has been proposed that drugs able to affect the cell cycle could enhance viral oncolysis by modulating viral gene expression (25). Lovastatin together with other clinically used statins (fluvastatin and simvastatin) induces a G_1 arrest of prostate cancer cells (26). A block of the cell cycle in ATC cells could enhance viral gene expression and increase the replication of *dl*1520. Further studies are required to clarify the mechanisms responsible for the effects of lovastatin on *dl*1520 gene expression and replication.

The administration of lovastatin *per os* to nude mice bearing ATC tumor xenografts enhances the antitumoral effects of *dl*1520 and increases the viral replication *in vivo*, confirming that this treatment could improve the clinical efficacy of replicating oncolytic adenoviruses. Interestingly, the injection of lovastatin and the virus within the tumor did not increase the effects of *dl*1520 (data not shown), indicating that a constant lovastatin blood concentration should be obtained to enhance the effects of *dl*1520.

The data presented here identify lovastatin as a promising agent for increasing the effects of oncolytic adenoviruses in ATC cells. It has been reported that FR901228 and trichostatin A, members of a new group of anticancer agents, the histone deacetylase inhibitors (27–29), or the MEK inhibitors U0126 and PD184352 (18) increase the antineoplastic effects of oncolytic adenoviruses. However, these agents have been used in a limited number of clinical trials, whereas 3-hydroxy-3-methylglutaryl coenzyme A reductase inhibitors have been widely used to reduce cardiovascular diseases without major adverse effects (10, 11). Lovastatin is generally well tolerated; the most important adverse effect is myotoxicity within the first 3 months of therapy (11). The risk of muscle dysfunction is increased by coadministration of other drugs able to interfere with lovastatin metabolism (11).

In the present study, in *in vitro* experiments, lovastatin was

used at final concentrations ranging from 2.5 to 10 μM, and in *in vivo*, we used a lovastatin concentration of 10 mg/kg/d.

Although the therapeutic dose for the treatment of hypercholesterolemia is about 1 mg/kg/d, which yields serum levels of 0.1 μM, it has been shown that serum concentrations of 2–4 μM of lovastatin are well tolerated in animal models, and clinical trials of phase I and II have been performed using 25 mg/kg/d with encouraging results (11). All these data indicate that lovastatin at a dose of 10 mg/kg/d could probably be used in ATC patients in combination with *dl*1520 without major side effects.

In conclusion, we have identified lovastatin as a drug that increases adenoviral replication and enhances the effects of an oncolytic adenovirus *in vitro* and *in vivo* against ATC cells. Therefore, lovastatin could be useful in the context of gene therapy for anaplastic thyroid carcinoma. Further studies are required to confirm the feasibility of this approach in ATC patients.

Acknowledgments

We thank Professor G. Vecchio and Dr. P. Formisano for their suggestions and a critical review of the manuscript. We thank Dr. G. Hallden for providing RmcB antibody. We also thank S. Sequino for technical assistance.

Received June 8, 2007. Accepted August 2, 2007.

Address all correspondence and requests for reprints to: Giuseppe Portella, Dipartimento di Biologia e Patologia Cellulare e Molecolare, Università di Napoli Federico II, via S. Pansini 5, 80131 Napoli, Italy. E-mail: portella@unina.it.

This work was supported by the Italian Ministry of Instruction, University, and Research (PRIN 2002) and the Associazione Italiana per la Ricerca sul Cancro.

Disclosure Statement: The authors have nothing to declare.

References

1. **Hedinger C, Williams ED, Sobin LH** 1989 The WHO histological classification of thyroid tumours: a commentary on the second edition. Cancer 63:908–911
2. **Ain KB** 2000 Management of undifferentiated thyroid cancer. Baillieres Best Pract Res Clin Endocrinol Metab 14:615–629
3. **Nikiforov YE** 2004 Genetic alterations involved in the transition from well-differentiated to poorly differentiated and anaplastic thyroid carcinomas. Endocr Pathol 15:319–327
4. **Sherman SI** 2003 Thyroid carcinoma. Lancet 361:501–511
5. **Parato KA, Senger D, Forsyth PA, Bell JC** 2005 Recent progress in the battle between oncolytic viruses and tumours. Nat Rev Cancer 12:965–976
6. **Kruyt FA, Curiel DT** 2002 Toward a new generation of conditionally replicating adenoviruses: pairing tumor selectivity with maximal oncolysis. Hum Gene Ther 13:485–495
7. **Post DE, Khuri FR, Simons JW, Van Meir EG** 2003 Replicative oncolytic adenoviruses in multimodal cancer regimens. Hum Gene Ther 14:933–946
8. **Portella G, Scala S, Vitagliano D, Vecchio G, Fusco A.** 2002 ONYX-015, an E1B gene-defective adenovirus, induces cell death in human anaplastic thyroid carcinoma cell lines. J Clin Endocrinol Metab 87:2525–2531
9. **Portella G, Pacelli R, Libertini S, Cella L, Vecchio G, Salvatore M, Fusco A** 2003 ONYX-015 enhances radiation-induced death of human anaplastic thyroid carcinoma cells. J Clin Endocrinol Metab 88:5027–5032
10. **Graaf MR, Richel DJ, Van Noorden CJ, Guchelaar HJ** 2004 Effects of statins and farnesyltransferase inhibitors on the development and progression of cancer. Cancer Treat Rev 30:609–641
11. **Chan KK, Oza AM, Siu LL**2003 The statins as anticancer agents. Clin Cancer Res 9:10–19
12. **Wang CY, Zhong WB, Chang TC, Lai SM, Tsai YF** 2003 Lovastatin, a 3-hydroxy-3-methylglutaryl coenzyme A reductase inhibitor, induces apoptosis and differentiation in human anaplastic thyroid carcinoma cells. J Clin Endocrinol Metab 88:3021–3026
13. **Zhong WB, Wang CY, Chang TC, Lee S** 2003 Lovastatin induces apoptosis of anaplastic thyroid cancer cells via inhibition of protein geranylgeranylation and *de novo* protein synthesis. Endocrinology 144:3852–3859
14. **Fiore L, Pollina LE, Fontani G, Casalone R, Berlingieri MT, Giannini R, Pacini F. Miccoli P, Toniolo A, Fusco A, Basolo F** 1997 Cytokine production by a new undifferentiated human thyroid carcinoma cell line, FB-1. J Clin Endocrinol Metab 82:4094–4100
15. **Skehan P, Storeng R, Scudiero D, Monks A, McMahon J, Vistica D, Warren J T, Bokesch H, Kenney S, Boyd MR** 1990 New colorimetric cytoxicity assay for anticancer-drug screening. J Natl Cancer Inst 82:1107–1112
16. **Abou El Hassan MA, Braam SR, Kruyt FA** 2006 Paclitaxel and vincristine potentiate adenoviral oncolysis that is associated with cell cycle and apoptosis modulation, whereas they differentially affect the viral life cycle in non-small-cell lung cancer cells. Cancer Gene Ther 12:1105–1114
17. **Hsu LK, Lonberg-Holm K, Alstein B, Crowell RL** 1988 A monoclonal antibody specific for the cellular receptor for the group B coxsackieviruses. J Virol 62:1647–1652
18. **Coyne CB, Bergelson JM** 2005 CAR: a virus receptor within the tight junction. Adv Drug Deliv Rev 57:869–882
19. **Anders M, Christian C, McMahon M, McCormick F, Korn WM** 2003 Inhibition of the Raf/MEK/ERK pathway up-regulates expression of the Coxsackie virus and adenovirus receptor in cancer cells. Cancer Res 63:2088–2095
20. **Crompton AM, Kirn DH** 2007 From ONYX-015 to armed vaccinia viruses: the education and evolution of oncolytic virus development. Curr Cancer Drug Targets 2:133–2139
21. **Marsee DK, Vadysirisack DD, Morrison CD, Prasad ML, Eng C, Duh QY, Rauen KA, Kloos RT, Jhiang SM** 2005 Variable expression of Coxsackie-adenovirus receptor in thyroid tumors: implications for adenoviral gene therapy. Thyroid 15:977–987
22. **Lacher MD, Tiirikainen MI, Saunier EF, Christian C, Anders M, Oft M, Balmain, A, Akhurst RJ, Korn WM** 2006 Transforming growth factor-beta receptor inhibition enhances adenoviral infectability of carcinoma cells via up-regulation of Coxsackie and adenovirus receptor in conjunction with reversal of epithelial-mesenchymal transition. Cancer Res 66:1648–1657
23. **Zhong WB, Liang YC, Wang CY, Chang TC, Lee WS** 2005 Lovastatin suppresses invasiveness of anaplastic thyroid cancer cells by inhibiting Rho geranylgeranylation and RhoA/ROCK signalling. Endocr Relat Cancer 3:615–629
24. **Li E, Brown SL, Stupack DG, Puente XS, Cheresh DA, Nemerow GR** 2001 Integrin $\alpha(v)\beta(1)$ is an adenovirus coreceptor. J Virol 75:5405–5409
25. **Abou El Hassan MA, Braam SR, Kruyt FA** 2006 A real-time RT-PCR assay for the quantitative determination of adenoviral gene expression in tumor cells. J Virol Methods 133:53–61
26. **Sivaprasad U, Abbas T, Dutta A** 2006 Differential efficacy of 3-hydroxy-3-methylglutaryl CoA reductase inhibitors on the cell cycle of prostate cancer cells. Mol Cancer Ther 5:2310–2316
27. **Goldsmith ME, Kitazono M, Fok P, Aikou T, Bates S, Fojo T** 2003 The histone deacetylase inhibitor FK228 preferentially enhances adenovirus transgene expression in malignant cells. Clin Cancer Res 9:5394–5401
28. **Bieler A, Mantwill K, Dravits T, Bernshausen A, Glockzin G, Kohler-Vargas N, Lage H, Gansbacher B, Holm PS** 2006 Novel three-pronged strategy to enhance cancer cell killing in glioblastoma cell lines: histone deacetylase inhibitor, chemotherapy, and oncolytic adenovirus dl520. Hum Gene Ther 17: 55–70
29. **Dion LD, Goldsmith KT, Tang DC, Engler JA, Yoshida M, Garver Jr RI** 1997 Amplification of recombinant adenoviral transgene products occurs by inhibition of histone deacetylase. Virology 231:201–209

***Endocrinology* is published monthly by The Endocrine Society (http://www.endo-society.org), the foremost professional society serving the endocrine community.**